

Electric field effects in one-dimensional spin-1/2 $K_1 J_1 \Gamma_1 \Gamma'_1 K_2 J_2$ model with ferromagnetic Kitaev coupling

Wang Yang,¹ Helin Wang,¹ and Chao Xu^{2,3}

¹*School of Physics, Nankai University, Tianjin 300071, China*

²*Institute for Advanced Study, Tsinghua University, Beijing 100084, China*

³*Kavli Institute for Theoretical Sciences, University of Chinese Academy of Sciences, Beijing 100190, China*

We perform a systematic study on the effects of electric fields in the Luttinger liquid phase of the one-dimensional spin-1/2 $K_1 J_1 \Gamma_1 \Gamma'_1 K_2 J_2$ model in the region of ferromagnetic nearest-neighboring Kitaev coupling. We find that while electric fields along (1, 1, 1)-direction maintain the Luttinger liquid behavior, fields along other directions drive the system to a dimerized state. An estimation is made on how effective a (1, 1, 1)-field is for tuning the Luttinger parameter in real materials. Our work is useful for understanding the effects of electric fields in one-dimensional generalized Kitaev spin models, and provides a starting point for exploring the electric-field-related physics in two dimensions based on a quasi-one-dimensional approach.

I. INTRODUCTION

Kitaev materials are two-dimensional (2D) solid state systems^{1–24} that are considered to be potentially useful for realizing Kitaev spin-1/2 model²⁵ on the honeycomb lattice, which is a prototypical exactly solvable model for realizing topological quantum computation^{25,26}. Iridates and α -RuCl₃ are typical Kitaev materials on the honeycomb lattice, which both have a ferromagnetic (FM) Kitaev coupling. Although the exactly solvable Kitaev model is a spin liquid model without any magnetic order, existing Kitaev materials are all magnetically ordered at sufficiently low temperatures^{27–30}, including zigzag, counter-rotating spiral and triple-Q orders, which hinder their applications for the purpose of topological quantum computing.

A central theme in the field of Kitaev materials is to find a method that can tune the real materials into the Kitaev spin liquid phase. Electric and magnetic controls are common and convenient controls of 2D materials. For example, experiments have found evidence that certain Kitaev materials exhibit half-quantized Hall conductance when external magnetic fields are applied above a critical value^{15,31–33}, which is a hallmark of the Kitaev spin liquid phase. On the other hand, electric field tuning of Kitaev materials remains much less explored in experiments.

On the theory side, the deviations of Kitaev materials away from the idealized spin liquid behaviors have been identified to originate from the existence of non-Kitaev coupling in real materials, including Heisenberg coupling^{1,2}, the off-diagonal Gamma and Γ' couplings⁶, and beyond nearest-neighboring interactions. Models that include these additional couplings are termed as generalized Kitaev models. For example, theories and experiments have revealed that the couplings satisfy $(K_1 < 0, J_1 > 0, \Gamma_1 > 0)$ in honeycomb iridates and $(K_1 < 0, J_1 < 0, \Gamma_1 > 0)$ in α -RuCl₃³⁴, where K_1 , J_1 and Γ_1 denote the nearest neighboring Kitaev, Gamma, and Heisenberg interactions, respectively. However, theoretical and numerical studies of generalized Kitaev models are very demanding because of their strongly correlated

nature.

In view of the aforementioned difficulties in 2D, a productive route is to study decoupled chains as a first step, leaving inter-chain interactions for a subsequent perturbative treatment. The 1D systems have the particular advantage that they are usually amenable for both analytical and numerical studies, because of various powerful 1D methods^{35–44} including bosonization, conformal field theory, and density matrix renormalization group (DMRG) numerics. Along this line, there have been surging research interests in 1D generalized Kitaev spin models^{45–62}, particularly focusing on effects of the bond-dependent Kitaev coupling and the off-diagonal Gamma coupling^{62–72}. Rich strongly correlated physics have been revealed in 1D Kitaev and Gamma models, including nonsymmorphic symmetries⁵⁸, emergent SU(2)₁ conformal invariance^{49,56}, exotic symmetry breaking phases, chiral soliton states^{73,74}, topological domain-wall excitations⁷⁵, and Lifshitz-type quantum phase transitions^{62,68,71}. It is also worth mentioning that besides providing hints for 2D physics, 1D studies have their independent merits as well, since experiments have established the existence of real 1D Kitaev materials^{76,77}.

Regarding electromagnetic controls in 1D, existing theoretical works in generalized Kitaev spin chains and ladders have been mostly focusing on magnetic fields^{73,78–83}, with electric fields much less explored. In Ref. 56, the authors studied the effects of electric fields along the third direction in spin-1/2 Kitaev-Gamma chain in the limit of vanishing Hund's coupling, where the first and second directions refer to the two bond directions in the decoupled 1D model, and the third direction is essentially the bond direction for inter-chain couplings within the parent 2D lattice. A systematic study of electric fields along general directions in more realistic models is still lacking.

In this work, we make a comprehensive study on the effects of static and uniform electric fields in 1D spin-1/2 $K_1 J_1 \Gamma_1 \Gamma'_1 K_2 J_2$ model in the $(K_1 < 0, J_1 > 0, \Gamma_1 > 0)$ region, where the subscripts “1” and “2” in $K_1 J_1 \Gamma_1 \Gamma'_1 K_2 J_2$ are used to denote nearest and second-nearest neighboring couplings, respectively. The chosen parameter range

is relevant for honeycomb iridates³⁴, and the model under consideration is a realistic one which includes up to second-nearest-neighboring interactions. In the absence of electric fields, the low energy physics of the 1D system can be described by Luttinger liquid theory when the Γ'_1, K_2, J_2 interactions are small enough, which are indeed much smaller than the K_1, J_1, Γ_1 couplings in real materials.

For nonzero electric fields, we analyze the effects of the fields using a field theory perturbation based on the $SU(2)_1$ Wess-Zumino-Witten (WZW) model. We find that the $(1, 1, 1)$ -direction is special: The system always remains in the Luttinger liquid phase when an electric field along the $(1, 1, 1)$ -direction is applied, as long as the field is not so large that it goes beyond the perturbative region. An estimation is made on how effective it is to use a $(1, 1, 1)$ -electric-field for tuning the Luttinger parameter in real materials. For all other directions of the electric fields, the system in general is driven into a dimerized state. Exceptions are electric fields along $(0, 0, 1)$ - and $(1, 1, 0)$ -directions in the limit of vanishing Hund's coupling, under which circumstances the system retains its Luttinger liquid behavior. Analytical predictions are all consistent with our large-scale DMRG numerical simulations.

The rest of the paper is organized as follows. Sec. II gives the expressions for the Hamiltonian of the $K_1 J_1 \Gamma_1 \Gamma'_1 K_2 J_2$ model and the couplings induced by the electric fields. Sec. III includes the expressions of the interactions in the Hamiltonian induced by electric fields. In Sec. IV, the low energy field theory of the model in the absence of electric fields is briefly reviewed, which provides a perturbative starting point for analyzing the effects of nonzero electric fields. Sec. V discusses in details the effects of electric fields in various directions based on field theory perturbation, which are confirmed numerically by DMRG simulations. Sec. VI summarizes the main results of the paper.

II. MODEL HAMILTONIAN

In this section, we give the expression for the Hamiltonian of the spin-1/2 $K_1 J_1 \Gamma_1 \Gamma'_1 K_2 J_2$ chain. A useful unitary transformation called six-sublattice rotation is defined, and symmetries of the model are discussed.

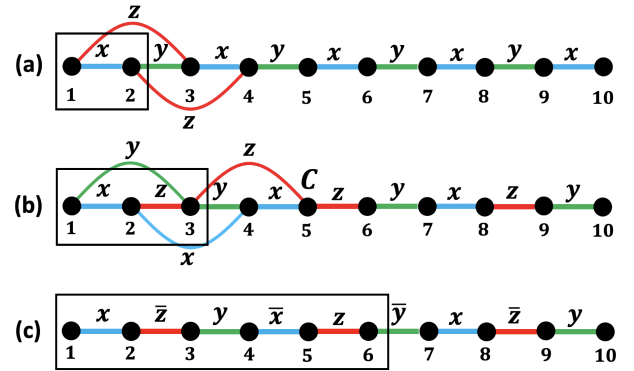


FIG. 1: Bond patterns of (a) the $K_1 J_1 \Gamma_1 \Gamma'_1 K_2 J_2$ chain without sublattice rotation, (b) the $K_1 J_1 \Gamma_1 \Gamma'_1 K_2 J_2$ chain after the six-sublattice rotation, (c) couplings induced by electric fields after the six-sublattice rotation. Black squares represent unit cells for the bond patterns.

A. The generalized Kitaev spin-1/2 chain

The Hamiltonian of the spin-1/2 $K_1 J_1 \Gamma_1 \Gamma'_1 K_2 J_2$ chain is defined as

$$H = \sum_{\langle ij \rangle \in \gamma \text{ bond}} [K_1 S_i^\gamma S_j^\gamma + J_1 \vec{S}_i \cdot \vec{S}_j + \Gamma_1 (S_i^\alpha S_j^\beta + S_i^\beta S_j^\alpha) + \Gamma'_1 (S_i^\gamma S_j^\alpha + S_i^\alpha S_j^\gamma + S_i^\gamma S_j^\beta + S_i^\beta S_j^\gamma)] + \sum_{\langle\langle ij \rangle\rangle} [K_2 S_i^z S_j^z + J_2 \vec{S}_i \cdot \vec{S}_j], \quad (1)$$

in which $\langle ij \rangle$ and $\langle\langle ij \rangle\rangle$ are used to denote nearest and second nearest neighboring sites i and j , respectively; the bond pattern for $\gamma \in \{x, y\}$ is shown in Fig. 1 (a), α, β are the two spin directions among $\{x, y, z\}$ other than γ , and (γ, α, β) forms a right-handed system. Third-nearest neighboring terms are not included in the 1D model in Eq. (1), since in 2D honeycomb lattice, there is only inter-chain but no intra-chain couplings in the leading third-nearest neighboring terms.

In what follows, we parametrize K_1, J_1, Γ_1 as

$$\begin{aligned} K_1 &= \sin(\theta) \cos(\phi) \\ \Gamma_1 &= \sin(\theta) \sin(\phi) \\ J_1 &= \cos(\theta). \end{aligned} \quad (2)$$

The condition $(K_1 < 0, \Gamma_1 > 0, J_1 > 0)$ is equivalent to $(0 < \theta < \pi/2, \pi/2 < \phi < \pi)$. As discussed in Appendix A 2, a typical set of values for the couplings $K_1, J_1, \Gamma_1, \Gamma'_1, J_2, K_2$ in iridates can be chosen as

$$\begin{aligned} \theta &= 0.44\pi \\ \phi &= 0.85\pi \\ \Gamma'_1 &= 0.1 \\ K_2 &= 0.02 \\ J_2 &= 0.2, \end{aligned} \quad (3)$$

in which the normalization is chosen as $K_1^2 + J_1^2 + \Gamma_1^2 = 1$ in accordance with Eq. (2) and the unit for the couplings is on the order of 10 meV. We will use the numbers in Eq. (3) for our DMRG numerical simulations in this work. We note that although Eq. (3) does not give the precise value of the couplings in real materials, the relative orders of magnitude of the couplings are captured by the chosen numerical numbers Eq. (3).

It is straightforward to verify that the Hamiltonian in Eq. (1) is invariant under the following symmetry transformations,

1. T : $(S_i^x, S_i^y, S_i^z) \rightarrow (-S_i^x, -S_i^y, -S_i^z)$
2. $T_a I_0$: $(S_i^x, S_i^y, S_i^z) \rightarrow (S_{-i+1}^x, S_{-i+1}^y, S_{-i+1}^z)$
3. $R(\hat{n}_N, \pi) T_a$: $(S_i^x, S_i^y, S_i^z) \rightarrow (-S_{i+1}^y, -S_{i+1}^x, -S_{i+1}^z)$

(4)

in which T is time reversal, T_{na} ($n \in \mathbb{Z}$) is spatial translation by n sites, I_0 is spatial inversion with inversion center at site 0, $R(\hat{n}, \theta)$ is global spin rotation around \hat{n} -axis with angle θ , and $\hat{n}_N = \frac{1}{\sqrt{2}}(1, -1, 0)$. The symmetry group G of the system is generated by the symmetry operations in Eq. (4) as

$$G = \langle T, T_a I_0, R(\hat{n}_N, \pi) T_a \rangle. \quad (5)$$

Notice in particular that the two-site translation $T_{2a} = [R(\hat{n}_N, \pi) T_a]^2$ is an element of G .

B. Six-sublattice rotation

In real materials, the magnitudes of the coupling constants usually satisfy the following hierarchy

$$|K_2|, |J_2|, |\Gamma'_1| \ll |J_1| \ll |K_1|, |\Gamma_1|. \quad (6)$$

Therefore, a good analytical strategy is to start with the nearest neighboring Kitaev-Gamma model, and then treat Heisenberg term J_1 as a perturbation, with small corrections from Γ'_1, K_2, J_2 terms. However, the Γ_1 term has a rather complicated off-diagonal form, involving interactions between spin operators along different directions. Therefore, a unitary transformation which maps the Γ_1 term to a diagonal form will be helpful for simplifying the analysis of the Γ_1 term. It turns out that such a unitary transformation indeed exists, acting as different spin rotations on different sites with a six-site periodicity, which we discuss below.

The six-sublattice rotation U_6 is defined as

- Sublattice 1 : $(x, y, z) \rightarrow (-x', -y', z')$,
- Sublattice 2 : $(x, y, z) \rightarrow (x', z', -y')$,
- Sublattice 3 : $(x, y, z) \rightarrow (-y', -z', x')$,
- Sublattice 4 : $(x, y, z) \rightarrow (y', x', -z')$,
- Sublattice 5 : $(x, y, z) \rightarrow (-z', -x', y')$,
- Sublattice 6 : $(x, y, z) \rightarrow (z', y', -x')$,

(7)

in which "Sublattice i " ($1 \leq i \leq 6$) represents all the sites $i + 6n$ ($n \in \mathbb{Z}$) in the chain, and we have abbreviated S^α (S'^α) as α (α') for short ($\alpha = x, y, z$). After the six-sublattice rotation, the Hamiltonian in Eq. (1) becomes

$$\begin{aligned} H' = & \sum_{\langle ij \rangle \in \gamma \text{ bond}} [-K_1 S_i'^\gamma S_j'^\gamma + \Gamma_1 (S_i'^\alpha S_j'^\alpha + S_i'^\beta S_j'^\beta) \\ & - J_1 (S_i'^\gamma S_j'^\gamma + S_i'^\alpha S_j'^\beta + S_i'^\beta S_j'^\alpha)] \\ & - \sum_{\langle\langle ij \rangle\rangle \in \gamma_2 \text{ bond}} \Gamma'_1 [(S_i'^\gamma S_j'^\alpha - S_i'^\alpha S_j'^\gamma) - (S_i'^\gamma S_j'^\beta - S_i'^\beta S_j'^\gamma)] \\ & + \sum_{\langle\langle ij \rangle\rangle \in \gamma_2 \text{ bond}} [K_2 S_i'^{\alpha_2} S_j'^{\beta_2} \\ & + J_2 (S_i'^x S_j'^y + S_i'^y S_j'^z + S_i'^z S_j'^x)], \end{aligned} \quad (8)$$

in which the nearest-neighboring bond γ and next-nearest-neighboring bond γ_2 have a three-site periodicity as shown in Fig. 1 (b), and both (γ, α, β) and $(\gamma_2, \alpha_2, \beta_2)$ form right-handed coordinate systems.

C. Symmetries

It can be verified that the Hamiltonian in Eq. (8) is invariant under the following symmetry transformations,

1. T : $(S_i^x, S_i^y, S_i^z) \rightarrow (-S_i^x, -S_i^y, -S_i^z)$
2. $R_a T_a$: $(S_i^x, S_i^y, S_i^z) \rightarrow (S_{i+1}^z, S_{i+1}^x, S_{i+1}^y)$
3. $R_I I_2$: $(S_i^x, S_i^y, S_i^z) \rightarrow (-S_{4-i}^z, -S_{4-i}^y, -S_{4-i}^x)$, (9)

in which I_2 is the spatial inversion with inversion center at site 2 in Fig. 1 (b); and $R_a = R(\hat{z}'', -2\pi/3)$, $R_I = R(\hat{y}'', \pi)$ where \hat{x}'', \hat{y}'' and \hat{z}'' are related to \hat{x}', \hat{y}' and \hat{z}' via

$$(\hat{x}'' \hat{y}'' \hat{z}'') = (\hat{x}' \hat{y}' \hat{z}') O, \quad (10)$$

in which the orthogonal matrix O is defined as

$$O = \begin{pmatrix} \frac{1}{\sqrt{6}} & \frac{1}{\sqrt{2}} & \frac{1}{\sqrt{3}} \\ -\sqrt{\frac{2}{3}} & 0 & \frac{1}{\sqrt{3}} \\ \frac{1}{\sqrt{6}} & -\frac{1}{\sqrt{2}} & \frac{1}{\sqrt{3}} \end{pmatrix}. \quad (11)$$

We will call the coordinate frame after the O transformation superimposed on the U_6 transformation as the OU_6 frame. Throughout this work, \tilde{S}_i , \tilde{S}'_i , and \tilde{S}''_i will be used to denote the spin operators in the original, U_6 , and OU_6 frames, respectively.

The symmetry group G' of the Hamiltonian H' in Eq. (9) is generated by the symmetry operations in Eq. (9) as

$$G' = \langle T, R_a T_a, R_I I_2 \rangle. \quad (12)$$

Notice that the symmetry groups G and G' must be related by the six-sublattice rotation U_6 . Indeed, the generators of G and G' are related by

$$\begin{aligned} U_6^{-1} R_a T_a U_6 &= R(\hat{n}_N, \pi) T_a \\ U_6^{-1} R_I I_2 U_6 &= T_{2a}^{-1} \cdot R(\hat{n}_N, \pi) T_a \cdot T_a I_0. \end{aligned} \quad (13)$$

III. COUPLINGS INDUCED BY ELECTRIC FIELDS

In this section, we give the expressions of the spin interactions induced by electric fields, and discuss the transformation properties of the electric fields under symmetry operations.

A. Dzyaloshinskii-Moriya interaction induced by electric fields

In Kitaev materials, Dzyaloshinskii-Moriya interactions can be induced by applying electric fields. Consider bond γ connecting nearest neighboring sites i, j , and the right-handed coordinate system (γ, α, β) . An electric field is called in-plane if its direction is within the $\alpha\beta$ -plane, and out-of-plane if it is parallel with the γ -axis. As shown in Ref. 84, an in-plane electric field induces a Dzyaloshinskii-Moriya interaction on bond γ in Fig. 1 (a) of the form

$$D_M^{(\text{in})} \hat{\gamma} \cdot (\vec{S}_i \times \vec{S}_j), \quad (14)$$

in which

$$D_M^{(\text{in})} = \lambda_{D+}^{(\text{in})}(E_\alpha + E_\beta) + \lambda_{D-}^{(\text{in})}(E_\alpha - E_\beta), \quad (15)$$

where E_α and E_β are the electric field components along the α - and β -directions. On the other hand, an out-of-plane electric field leads to the following interaction on the γ bond⁸⁴

$$D_M^{(\text{out})} (\hat{\alpha} + \hat{\beta}) \cdot (\vec{S}_i \times \vec{S}_j) + \Gamma'^{(\text{out})} [S_i^\gamma (S_j^\alpha + S_j^\beta) + (S_i^\alpha + S_i^\beta) S_j^\gamma], \quad (16)$$

in which

$$\begin{aligned} D_M^{(\text{out})} &= \lambda_D^{(\text{out})} E_\gamma, \\ \Gamma'^{(\text{out})} &= \lambda_\Gamma^{(\text{out})} E_\gamma. \end{aligned} \quad (17)$$

In Eq. (15,17), $\lambda_{D+}^{(\text{in})}, \lambda_{D-}^{(\text{in})}, \lambda_D^{(\text{out})}, \lambda_\Gamma^{(\text{out})}$ are related to microscopic parameters including on-site Hubbard interactions, hopping integrals, energy differences between different orbitals, and Hund's coupling, as derived from Ref. 84. Detailed expressions are included in Appendix A.

An estimation of order of magnitudes of the coupling constants in iridates is given in Appendix A 2. In accordance with the discussions in Appendix A 2, by setting the unit for electric fields as eV/nm, a typical set of values for $\lambda_{D+}^{(\text{in})}, \lambda_{D-}^{(\text{in})}, \lambda_D^{(\text{out})}, \lambda_\Gamma^{(\text{out})}$ can be taken as

$$\begin{aligned} \lambda_{D+}^{(\text{in})} &= -0.1 \\ \lambda_{D-}^{(\text{in})} &= -0.05 \\ \lambda_D^{(\text{out})} &= 0.04 \\ \lambda_\Gamma^{(\text{out})} &= 0.05, \end{aligned} \quad (18)$$

which will be used in numerical calculations in this work. Again we note that Eq. (18) does not give the precise values of the coupling constants in real materials, but give the correct order of magnitudes.

B. Couplings in six-sublattice-rotated frame

In the six-sublattice rotated frame, the couplings induced by electric fields are six-site periodic, different from H' in Eq. (8) having a three-site periodicity. In what follows, we use $\tilde{\gamma} \in \{x, y, z, \bar{x}, \bar{y}, \bar{z}\}$ to denote the bond for couplings involving electric fields, where the bond pattern for $\tilde{\gamma}$ is shown in Fig. 1 (c). Similar as before, $\tilde{\alpha}, \tilde{\beta}$ are defined as the two spin directions complementary to the direction associated with $\tilde{\gamma}$, and $(\tilde{\gamma}, \tilde{\alpha}, \tilde{\beta})$ form a right-handed coordinate system.

As can be verified, after performing the six-sublattice rotation, an in-plane electric field in Eq. (14) induces a coupling on bond $\tilde{\gamma}$ in Fig. 1 (c) as

$$(-)^{i-1} D_M^{(\text{in})} (-S_i'^{\tilde{\alpha}} S_j'^{\tilde{\alpha}} + S_i'^{\tilde{\beta}} S_j'^{\tilde{\beta}}), \quad (19)$$

whereas an out-of-plane electric field in Eq. (16) induces a coupling on bond $\tilde{\gamma}$ as

$$\begin{aligned} &(-)^i D_M^{(\text{out})} [(S_i'^{\tilde{\gamma}} S_j'^{\tilde{\alpha}} - S_i'^{\tilde{\alpha}} S_j'^{\tilde{\gamma}}) + (S_i'^{\tilde{\gamma}} S_j'^{\tilde{\beta}} - S_i'^{\tilde{\beta}} S_j'^{\tilde{\gamma}})] \\ &- \Gamma'^{(\text{out})} [(S_i'^{\tilde{\gamma}} S_j'^{\tilde{\alpha}} - S_i'^{\tilde{\alpha}} S_j'^{\tilde{\gamma}}) - (S_i'^{\tilde{\gamma}} S_j'^{\tilde{\beta}} - S_i'^{\tilde{\beta}} S_j'^{\tilde{\gamma}})]. \end{aligned} \quad (20)$$

C. Symmetry transformations of electric fields

To facilitate symmetry analysis in later sections, we discuss in details how electric field terms transform under symmetry operations. We will be interested in symmetry transformation properties in the six-sublattice rotated frame.

We introduce the following terms in the six-sublattice rotated frame,

$$\begin{aligned} \mathcal{H}'^{(\text{in})}_{D,\text{odd/even}} &= \sum_{\substack{\langle ij \rangle \in \tilde{\gamma} \text{ bond} \\ i \in \text{odd/even}}} (-)^{i-1} (-S_i'^{\tilde{\alpha}} S_j'^{\tilde{\alpha}} + S_i'^{\tilde{\beta}} S_j'^{\tilde{\beta}}) \\ \mathcal{H}'^{(\text{out})}_{D,\text{odd/even}} &= \sum_{\substack{\langle ij \rangle \in \tilde{\gamma} \text{ bond} \\ i \in \text{odd/even}}} (-)^i [(S_i'^{\tilde{\gamma}} S_j'^{\tilde{\alpha}} - S_i'^{\tilde{\alpha}} S_j'^{\tilde{\gamma}}) + (S_i'^{\tilde{\gamma}} S_j'^{\tilde{\beta}} - S_i'^{\tilde{\beta}} S_j'^{\tilde{\gamma}})] \\ \mathcal{H}'^{(\text{out})}_{\Gamma,\text{odd/even}} &= \sum_{\substack{\langle ij \rangle \in \tilde{\gamma} \text{ bond} \\ i \in \text{odd/even}}} [-(S_i'^{\tilde{\gamma}} S_j'^{\tilde{\alpha}} - S_i'^{\tilde{\alpha}} S_j'^{\tilde{\gamma}}) + (S_i'^{\tilde{\gamma}} S_j'^{\tilde{\beta}} - S_i'^{\tilde{\beta}} S_j'^{\tilde{\gamma}})]. \end{aligned} \quad (21)$$

It is enough to consider how they transform under generators of the symmetry group G' in Eq. (12). The couplings in Eq. (21) are apparently invariant under time

reversal operation. Their transformation properties under $R_a T_a$ and $R_I I_2$ can be derived as (for details, see Appendix C)

$$\begin{aligned} R_a T_a : \mathcal{H}_{D,\text{odd}}^{\prime(\text{in})} &\longleftrightarrow -\mathcal{H}_{D,\text{even}}^{\prime(\text{in})} \\ \mathcal{H}_{D,\text{odd}}^{\prime(\text{out})} &\longleftrightarrow -\mathcal{H}_{D,\text{even}}^{\prime(\text{out})} \\ \mathcal{H}_{\Gamma,\text{odd}}^{\prime(\text{out})} &\longleftrightarrow \mathcal{H}_{\Gamma,\text{even}}^{\prime(\text{out})}, \end{aligned} \quad (22)$$

and

$$\begin{aligned} R_I I_2 : \mathcal{H}_{D,\text{odd}}^{\prime(\text{in})} &\longleftrightarrow \mathcal{H}_{D,\text{even}}^{\prime(\text{in})} \\ \mathcal{H}_{D,\text{odd}}^{\prime(\text{out})} &\longleftrightarrow \mathcal{H}_{D,\text{even}}^{\prime(\text{out})} \\ \mathcal{H}_{\Gamma,\text{odd}}^{\prime(\text{out})} &\longleftrightarrow \mathcal{H}_{\Gamma,\text{even}}^{\prime(\text{out})}. \end{aligned} \quad (23)$$

IV. LOW ENERGY THEORY WITHOUT EXTERNAL FIELDS

In this section, we briefly review the low energy field theory of the model in Eq. (1) in the absence of electric fields, which provides a perturbative starting point for analyzing the effects of nonzero fields in later sections. Throughout this work, we will consider the parameter region $(K_1 < 0, \Gamma_1 > 0, J_1 > 0)$, which is relevant for honeycomb iridates. We follow the strategy mentioned at the beginning of Sec. II B, by considering the Kitaev-Gamma model first, then treating the Heisenberg coupling J_1 as a perturbation, and finally analyzing the effects of Γ'_1, J_2, K_2 .

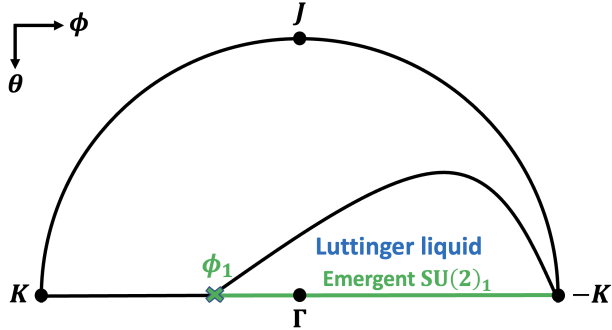


FIG. 2: Schematic plot of the Luttinger liquid phase of spin-1/2 $K_1 J_1 \Gamma_1$ model in the $(K_1 < 0, \Gamma_1 > 0, J_1 > 0)$ region, in which K_1, J_1, Γ_1 are parametrized by θ, ϕ in accordance with Eq. (2). The line marked with green color corresponds to Kitaev-Gamma model, which has an emergent $SU(2)_1$ conformal symmetry at low energies where the transition point ϕ_1 is 0.33π , as discussed in Ref. 49. The system remains in the Luttinger liquid phase in the $K_1 J_1 \Gamma_1 \Gamma'_1 K_2 J_2$ model for small enough Γ'_1, K_2, J_2 .

A. The Kitaev-Gamma model

Ref. 49 shows that in the $(K_1 < 0, \Gamma_1 > 0)$ region, the low energy physics of the 1D spin-1/2 Kitaev-Gamma

model in the six-sublattice rotated frame is described by the $SU(2)_1$ Wess-Zumino-Witten (WZW) model. The Hamiltonian of the $SU(2)_1$ WZW model is of the following Sugawara form

$$H_{\text{WZW}} = \int dx \left[\frac{2\pi}{3} v_0 (\vec{J}'_L \cdot \vec{J}'_L + \vec{J}'_R \cdot \vec{J}'_R) \right], \quad (24)$$

in which v_0 is the spin velocity; $\vec{J}'_L = -\frac{1}{4\pi} \text{tr}[(\partial_z g) g^\dagger \vec{\sigma}]$ and $\vec{J}'_R = \frac{1}{4\pi} \text{tr}[g^\dagger (\partial_z g) \vec{\sigma}]$ are the left and right WZW currents, respectively, where the $SU(2)$ matrix g is the WZW primary field, σ^α ($\alpha = x, y, z$) are the three Pauli matrices, and $z = \tau + ix$ ($\bar{z} = \tau - ix$) is the holomorphic (anti-holomorphic) coordinate in the imaginary time formalism. For the Kitaev-Gamma model, there exists an additional marginally irrelevant coupling in the low energy field theory, such that the low energy Hamiltonian becomes

$$H_{K_1 \Gamma_1}^{\text{Low}} = \int dx \left[\frac{2\pi}{3} v_0 (\vec{J}'_L \cdot \vec{J}'_L + \vec{J}'_R \cdot \vec{J}'_R) - u_0 \vec{J}'_L \cdot \vec{J}'_R \right], \quad (25)$$

where $u_0 > 0$ is the coupling constant of the marginally irrelevant term $\vec{J}'_L \cdot \vec{J}'_R$. For later convenience, we define dimerization fluctuation ϵ and Néel order parameter \vec{N}' in the U_6 frame as

$$\begin{aligned} \epsilon &= \text{tr}(g), \\ \vec{N}' &= \text{tr}(g \vec{\sigma}). \end{aligned} \quad (26)$$

B. The $K_1 J_1 \Gamma_1 \Gamma'_1 K_2 J_2$ model

1. The Kitaev-Heisenberg-Gamma model

In Ref. 50, it has been shown that in the $(K_1 < 0, \Gamma_1 > 0)$ parameter region with a small $J_1 > 0$ term, the Hamiltonian density of the $K_1 J_1 \Gamma_1$ model acquires the form

$$\begin{aligned} H_{K_1 J_1 \Gamma_1}^{\text{Low}} &= \int dx \left[\frac{2\pi}{3} v_1 (\vec{J}'_L \cdot \vec{J}'_L + \vec{J}'_R \cdot \vec{J}'_R) \right. \\ &\quad \left. + \nu_1 (J''_L^z - J''_R^z) - u_1 \vec{J}'_L \cdot \vec{J}'_R + u_{1z} J'_L^z J'_R^z \right], \end{aligned} \quad (27)$$

in which $J''_\lambda^z = \vec{J}'_\lambda \cdot \hat{z}''$ ($\lambda = L, R$) is along z'' -direction in the OU_6 -frame. The ν_1 term can be eliminated by a chiral rotation, which transforms the low energy Hamiltonian in Eq. (27) to

$$\begin{aligned} H_{K_1 J_1 \Gamma_1}^{\text{Low}} &= \int dx \left[\frac{2\pi}{3} \tilde{v}_1 (\vec{J}'_L \cdot \vec{J}'_L + \vec{J}'_R \cdot \vec{J}'_R) \right. \\ &\quad \left. - \tilde{u}_1 \vec{J}'_L \cdot \vec{J}'_R + \tilde{u}_{1z} J'_L^z J'_R^z \right], \end{aligned} \quad (28)$$

in which $\tilde{v}_1, \tilde{u}_1, \tilde{u}_{1z}$ are different from v_1, u_1, u_{1z} because of the chiral rotation. We note that for $\lambda_1 > 0$, the system has a Luttinger liquid behavior at low energies.

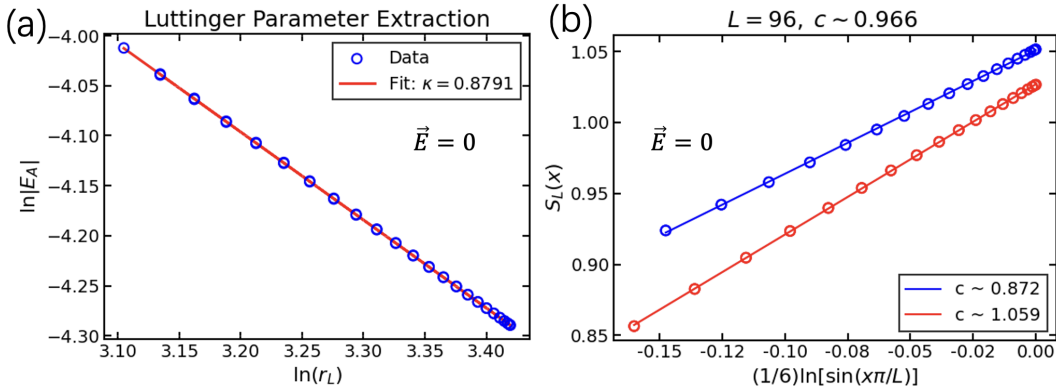


FIG. 3: (a) Staggered energy density $E_A(r)$ as a function of r_L on a log-log scale and (b) entanglement entropy $S_L(x)$ as a function of $\frac{1}{6} \sin(\frac{\pi x}{L})$ in the absence of electric fields, where $r_L = \frac{L}{\pi} \sin(\frac{\pi x}{L})$. In (a,b), DMRG numerics are performed on a system of $L = 96$ sites using open boundary conditions, with bond dimension m and truncation error ϵ chosen as $m = 1000$, $\epsilon = 10^{-10}$. The parameters of $K_1, J_1, \Gamma_1, \Gamma'_1, K_2, J_2$ in DMRG numerics are taken in accordance with Eq. (3) and Eq. (18).

Alternatively, in the language of Abelian bosonization, the low energy physics can be described by the following Luttinger liquid Hamiltonian

$$H_{LL} = \frac{v}{2} \int dx \left[\frac{1}{\kappa} (\nabla \varphi)^2 + \kappa (\nabla \theta)^2 \right], \quad (29)$$

in which the θ, φ fields satisfy the commutation relation $[\varphi(x), \theta(x')] = \frac{i}{2} \text{sgn}(x' - x)$, v is the velocity, and κ is the Luttinger liquid parameter. Notice that κ satisfies $\kappa = 0.5$ for $J = 0$ and $0.5 < \kappa < 1$ in the Luttinger liquid phase for $J > 0$, as revealed by DMRG numerics in Ref. 50. We also note that in the Luttinger liquid phase, the system has an emergent U(1) rotation symmetry around the \hat{z}'' -direction, which is expected from the symmetry operation $R_a T_a$ in Eq. (9).

2. General cases

Since the Luttinger liquid phase is derived from general symmetry and renormalization group (RG) analysis (as discussed in details in Ref. 50), the phase is stable against small perturbations. In particular, as long as Γ', K_2, J_2 are small enough, the system remains in the same Luttinger liquid phase.

C. DMRG numerics

The behavior of the energy density can be used as a test for Luttinger liquids. In the Luttinger liquid phase, the energy density $E(r) = \langle H_r \rangle$ can be separated into a uniform component $E_U(r)$ and a staggered component $E_A(r)$ in the long distance limit $r \gg 1$ if open boundary conditions are used, i.e.,

$$E(r) = E_U(r) + (-)^r E_A(r), \quad (30)$$

in which r is the distance measured from one of the two boundaries of the system, H_r is the sum of the terms in the Hamiltonian starting with site r , $\langle H_r \rangle$ is the ground state expectation value of H_r , and both $E_U(r)$ and $E_A(r)$ are smooth functions of r on a length scale much larger than the lattice constant. In the Luttinger liquid phase, $E_A(r)$ is predicted to behave in the long distance limit as⁸⁵

$$E_A(r) \propto (r_L)^{-\kappa}, \quad (31)$$

in which κ is the Luttinger parameter, and

$$r_L = \frac{L}{\pi} \sin\left(\frac{\pi r}{L}\right). \quad (32)$$

The value of central charge can also serve as a test for Luttinger liquid behavior. The central charge can be extracted from calculating entanglement entropy⁸⁶. The entanglement entropy $S_L(x)$ for a subregion of length x in a finite chain of length L is predicted by conformal field theory (CFT) as⁸⁶

$$S_L(x) = \lambda \frac{c}{3} \ln \left[\frac{L}{\pi} \sin \left(\frac{\pi x}{L} \right) \right] + \dots, \quad (33)$$

in which c is the central charge, $\lambda = 1$ (and $1/2$) for periodic (and open) boundary conditions and “ \dots ” represents sub-leading terms in the long distance limit. In the Luttinger liquid phase, the central charge is predicted to be $c = 1$.

We have numerically calculated the energy density $E(r)$ and entanglement entropy $S_L(x)$ at zero electric field on a system of $L = 96$ sites with open boundary conditions. The parameters for $K_1, J_1, \Gamma_1, \Gamma'_1, K_2, J_2$ in DMRG simulations are chosen in accordance with Eq. (3). Fig. 3 (a) shows $E_A(r)$ as a function of r_L on a log-log scale, which exhibits a nearly perfect linear relation. The Luttinger parameter κ can be extracted from Fig.

3 (a) using Eq. (31), which gives $\kappa = 0.8791$. Fig. 3 (b) shows $S_L(x)$ as a function of $\frac{1}{6} \ln[\frac{L}{\pi} \sin(\frac{\pi x}{L})]$, which, apart from an oscillating behavior, also exhibits a linear relation. The central charge value can be determined as the average of the two slopes in Fig. 3 (b), which gives $c = 0.966$, being very close to 1.

V. EFFECTS OF ELECTRIC FIELDS

In this section, we investigate the effects of electric fields on Luttinger liquid behaviors of generalized Kitaev spin-1/2 chains.

An electric field along x -direction is out-of-plane (in-plane) on x - (y -) bonds; an electric field along y -direction is in-plane (out-of-plane) on x - (y -) bonds; and an electric field along z -direction is in-plane on both x - and y -bonds, where the bonds refer to those in Fig. 1 (a) in the unrotated frame. According to the formulas in Sec. III A, a uniform electric field $\vec{E} = (E_x, E_y, E_z)$ introduces the following terms in the six-sublattice rotated frame,

$$\begin{aligned} & r_1(\mathcal{H}_{D,\text{odd}}'^{(\text{in})} + \mathcal{H}_{D,\text{even}}'^{(\text{in})}) + r_2(\mathcal{H}_{D,\text{odd}}'^{(\text{in})} - \mathcal{H}_{D,\text{even}}'^{(\text{in})}) \\ & + r_3(\mathcal{H}_{D,\text{odd}}'^{(\text{out})} + \mathcal{H}_{D,\text{even}}'^{(\text{out})}) + r_4(\mathcal{H}_{D,\text{odd}}'^{(\text{out})} - \mathcal{H}_{D,\text{even}}'^{(\text{out})}) \\ & + r_5(\mathcal{H}_{\Gamma,\text{odd}}'^{(\text{out})} + \mathcal{H}_{\Gamma,\text{even}}'^{(\text{out})}) + r_6(\mathcal{H}_{\Gamma,\text{odd}}'^{(\text{out})} - \mathcal{H}_{\Gamma,\text{even}}'^{(\text{out})}), \end{aligned} \quad (34)$$

in which

$$\begin{aligned} r_1 &= \frac{1}{2}[\lambda_{D+}^{(\text{in})}(E_x + E_y + 2E_z) - \lambda_{D-}^{(\text{in})}(E_x - E_y)] \\ r_2 &= \frac{1}{2}[-\lambda_{D+}^{(\text{in})}(E_x - E_y) + \lambda_{D-}^{(\text{in})}(E_x + E_y - 2E_z)] \\ r_3 &= \frac{1}{2}\lambda_D^{(\text{out})}(E_x + E_y) \\ r_4 &= \frac{1}{2}\lambda_D^{(\text{out})}(E_x - E_y) \\ r_5 &= \frac{1}{2}\lambda_{\Gamma}^{(\text{out})}(E_x + E_y) \\ r_6 &= \frac{1}{2}\lambda_{\Gamma}^{(\text{out})}(E_x - E_y). \end{aligned} \quad (35)$$

A. Electric field along (1, 1, 1)-direction

We start with an electric field along (1, 1, 1)-direction, namely

$$\vec{E}_{111} = \frac{1}{\sqrt{3}}E_{111}(\hat{x} + \hat{y} + \hat{z}). \quad (36)$$

Using Eq. (34), the Hamiltonian $H'_{E,111}$ in the U_6 frame can be obtained as

$$\begin{aligned} H'_{E,111} &= H' + \frac{1}{\sqrt{3}}E_{111}[2\lambda_{D+}^{(\text{in})}(\mathcal{H}_{D,\text{odd}}'^{(\text{in})} + \mathcal{H}_{D,\text{even}}'^{(\text{in})}) \\ & + \lambda_D^{(\text{out})}(\mathcal{H}_{D,\text{odd}}'^{(\text{out})} + \mathcal{H}_{D,\text{even}}'^{(\text{out})}) + \lambda_{\Gamma}^{(\text{out})}(\mathcal{H}_{\Gamma,\text{odd}}'^{(\text{out})} + \mathcal{H}_{\Gamma,\text{even}}'^{(\text{out})})], \end{aligned} \quad (37)$$

where H' is given in Eq. (8).

1. Luttinger liquid behavior

According to the discussions in Sec. III C, it is straightforward to see that the symmetry group $G'_{E,111}$ of $H'_{E,111}$ in Eq. (37) is

$$G'_{E,111} = \langle T, R_a^{-1}T_{2a}, R_I I_2 \rangle. \quad (38)$$

Using the symmetry transformation properties in Eqs. (D1,D2,D3,D4), we perform a symmetry analysis to figure out the low energy field theory for the case of an electric field along (1, 1, 1)-direction. The $SU(2)_1$ WZW model in Eq. (24) is taken as the unperturbed system. For perturbations, in the sense of renormalization group flow, we will only keep relevant and marginal operators, which have scaling dimensions smaller than and equal to two.

For a symmetry analysis of the low energy theory, it turns out to be easier to work in the OU_6 frame, by defining \vec{J}'' and \vec{N}'' as

$$\begin{aligned} (J''^x, J''^y, J''^z) &= (J^x, J^y, J^z)O, \\ (N''^x, N''^y, N''^z) &= (N^x, N^y, N^z)O, \end{aligned} \quad (39)$$

in which O is defined in Eq. (11). All symmetry allowed relevant and marginal operators can be classified as follows.

- 1) $\epsilon = \text{tr}(g)$ is forbidden by $R_I I_2$.
- 2) N''^{α} ($\alpha = x, y, z$) is forbidden by T .
- 3) For $J''_{L/R}^{\alpha}$ ($\alpha = x, y, z$), time reversal requires the combination $J''_L^{\alpha} - J''_R^{\alpha}$. Then $R_a^{-1}T_{2a}$ requires $J''_L^z - J''_R^z$, which is invariant under $R_I I_2$.
- 4) For $J''_L^{\alpha}\epsilon, J''_R^{\alpha}\epsilon$ ($\alpha = x, y, z$), time reversal requires the combination $(J''_L^{\alpha} - J''_R^{\alpha})\epsilon$. Then $R_a^{-1}T_{2a}$ requires $(J''_L^z - J''_R^z)\epsilon$. However, $(J''_L^z - J''_R^z)\epsilon$ changes sign under $R_I I_2$, hence forbidden.
- 5) Within $J''_L^{\alpha}N''^{\beta}, J''_R^{\alpha}N''^{\beta}$, the terms allowed by T and $R_a^{-1}T_{2a}$ are $(\vec{J}_L'' + \vec{J}_R'') \cdot \vec{N}'$, $(J''_L^z + J''_R^z)N''^z$, and $(J''_L^x + J''_R^x)N''^y - (J''_L^y + J''_R^y)N''^x$, in which $(J''_L^x + J''_R^x)N''^y - (J''_L^y + J''_R^y)N''^x$ changes sign under $R_I I_2$, hence forbidden.
- 6) For $J''_L^{\alpha}J''_R^{\beta}$, the allowed terms by T and $R_a^{-1}T_{2a}$ are $\vec{J}_L'' \cdot \vec{J}_R'', J''_L^z J''_R^z$, and $J''_L^x J''_R^y - J''_L^y J''_R^x$, in which $J''_L^x J''_R^y - J''_L^y J''_R^x$ changes sign under $R_I I_2$, hence forbidden.

Hence, the low energy Hamiltonian is given by

$$\begin{aligned} H'_{E,111}^{\text{Low}} &= \frac{2\pi v_2}{3} \int dx (\vec{J}_L'' \cdot \vec{J}_L'' + \vec{J}_R'' \cdot \vec{J}_R'') \\ & + \nu_2 \int dx (J''_L^z - J''_R^z) \\ & + \lambda_2 \int dx (\vec{J}_L'' + \vec{J}_R'') \cdot \vec{N}' + \lambda_{2z} \int dx (J''_L^z + J''_R^z)N''^z \\ & - u_2 \int dx \vec{J}_L'' \cdot \vec{J}_R'' + u_{2z} \int dx J''_L^z J''_R^z, \end{aligned} \quad (40)$$

in which $v_2, \nu_2, u_2, u_{2z}, \lambda_2, \lambda_{2z}$ are the coupling constants of the corresponding terms. As discussed in Ref. 56, the

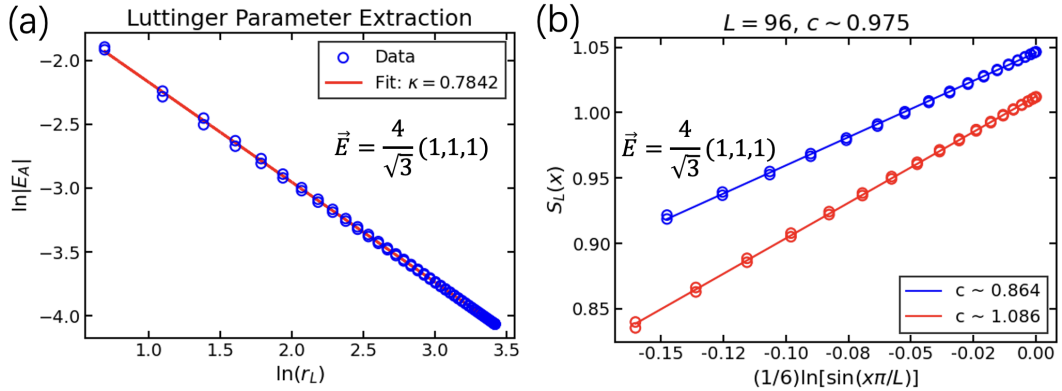


FIG. 4: (a) Staggered energy density $E_A(r)$ as a function of r_L on a log-log scale and (b) entanglement entropy $S_L(x)$ as a function of $\frac{1}{6} \sin(\frac{\pi x}{L})$ with electric field $\vec{E} = \frac{4}{\sqrt{3}}(1, 1, 1)$, where $r_L = \frac{L}{\pi} \sin(\frac{\pi x}{L})$. In (a,b), DMRG numerics are performed on a system of $L = 96$ sites using open boundary conditions, with bond dimension m and truncation error ϵ chosen as $m = 1000$, $\epsilon = 10^{-10}$. The parameters of $K_1, J_1, \Gamma_1, \Gamma'_1, K_2, J_2$ in DMRG numerics are taken in accordance with Eq. (3) and Eq. (18).

λ_2, λ_{2z} terms can be neglected since they are total derivatives, only contributing to boundary terms. Furthermore, the ν_2 term can be eliminated by a chiral rotation⁸⁷⁻⁸⁹. Removing the $\lambda_2, \lambda_{2z}, \nu_2$ terms, the low energy Hamiltonian becomes

$$H'_{E,111} = \frac{2\pi\tilde{v}_2}{3} \int dx (\vec{J}'_L \cdot \vec{J}'_L + \vec{J}'_R \cdot \vec{J}'_R) - \tilde{u}_2 \int dx \vec{J}'_L \cdot \vec{J}'_R + \tilde{u}_{2z} \int dx J''_L z J''_R z. \quad (41)$$

The low energy physics of $H'_{E,111}$ in Eq. (41) is the same as an easy-plane AFM XXZ model when $\tilde{u}_{2z} > 0$. Hence, for small enough E_z , the system remains in the Luttinger liquid phase.

2. Numerical results

We have calculated the staggered energy density $E_A(r)$ and entanglement entropy $S_L(x)$ for $\vec{E}_{111} = \frac{4}{\sqrt{3}}(1, 1, 1)$. DMRG calculations are performed on a system of $L = 96$ sites under open boundary conditions, with parameters $K_1, J_1, \Gamma_1, \Gamma'_1, K_2, J_2$ and $\lambda_{D+}^{(in)}, \lambda_{D-}^{(in)}, \lambda_D^{(out)}, \lambda_{\Gamma}^{(out)}$ chosen in accordance with Eq. (3) and Eq. (18). $E_A(r)$ vs. r_L on a log-log scale and $S_L(x)$ vs. $\frac{1}{6} \ln[\frac{L}{\pi} \sin(\frac{\pi x}{L})]$ are shown in Fig. 4 (a) and Fig. 4 (b), respectively. As can be seen from Fig. 4 (a,b), the DMRG numerical results for both fields are in good agreements with Luttinger liquid behaviors, giving a Luttinger parameter $\kappa = 0.7842$.

Therefore, we see that electric fields along $(1, 1, 1)$ -direction can be used as a method to tune the Luttinger parameter of the system. However, such tuning is not quite effective, at least in iridates. Comparing Fig. 3 (a) and Fig. 4 (a), the Luttinger parameter changes by 10.8% when $\vec{E} = \frac{4}{\sqrt{3}}(1, 1, 1)$ is applied, corresponding to $\sim 4 \times 10^9 \text{ V/m}$ according to the estimations in Sec. III A.

Notice that an 10^9 V/m electric field is already on the order of field values for intrinsic dielectric breakdown in iridate materials⁹⁰.

B. Electric field along z -direction

Next we consider an electric field along z -direction. Using Eq. (34), the Hamiltonian $H'_{E,z}$ in the U_6 frame can be obtained as

$$H'_{E,z} = H' + E_z \lambda_{D+}^{(in)} (\mathcal{H}_{D,odd}^{(in)} + \mathcal{H}_{D,even}^{(in)}) - E_z \lambda_{D-}^{(in)} (\mathcal{H}_{D,odd}^{(in)} - \mathcal{H}_{D,even}^{(in)}), \quad (42)$$

where H' is given in Eq. (8). Since $J_H \ll U_d, U_p$ in real materials, $\lambda_{D-}^{(in)}$ is smaller than $\lambda_{D+}^{(in)}$ according to Eq. (A1). Hence, we will study $\lambda_{D-}^{(in)} = 0$ first, and then treat $\lambda_{D-}^{(in)}$ as a small perturbation.

1. Luttinger liquid behavior for $\lambda_{D-}^{(in)} = 0$

If $J_H = 0$, we have $\lambda_{D-}^{(in)} = 0$, and the Hamiltonian $H'_{E,z0}$ is given by

$$H'_{E,z0} = H' + E_z \lambda_{D+}^{(in)} (\mathcal{H}_{D,odd}^{(in)} + \mathcal{H}_{D,even}^{(in)}), \quad (43)$$

where H' is the Hamiltonian for the spin-1/2 $K_1 J_1 \Gamma_1 \Gamma'_1 K_2 J_2$ model in the six-sublattice rotated frame given in Eq. (8). According to the discussions in Sec. III C, it can be straightforwardly verified that the symmetry group $G'_{E,z0}$ of $H'_{E,z0}$ in Eq. (43) is

$$G'_{E,z0} = \langle T, R_a^{-1} T_{2a}, R_I I_2 \rangle. \quad (44)$$

Since $G'_{E,z0}$ is the same as $G'_{E,111}$ in Eq. (38), the low energy field theory acquires the same form as Eq. (41).

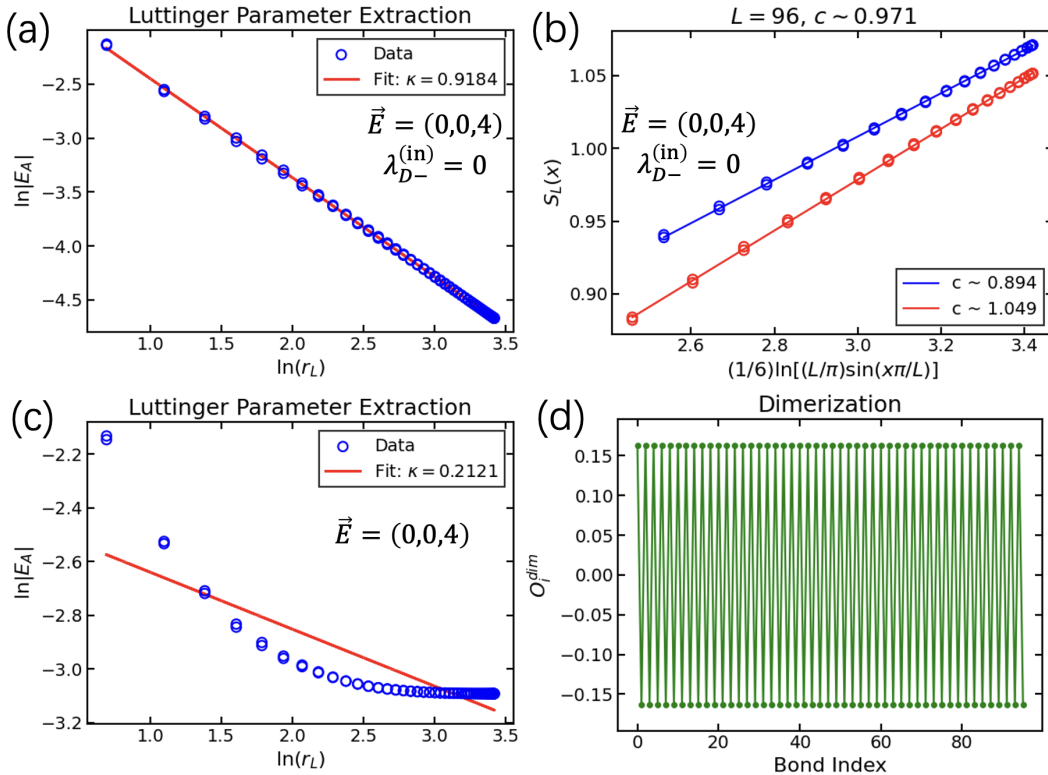


FIG. 5: (a) Staggered energy density $E_A(r)$ as a function of r_L on a log-log scale and (b) entanglement entropy $S_L(x)$ as a function of $\frac{1}{6} \sin(\frac{\pi x}{L})$ for $\vec{E} = (0, 0, 4)$ and $\lambda_{D-}^{(0)} = 0$, (c) staggered energy density $E_A(r)$ as a function of r_L on a log-log scale and (d) dimerization $O'_{\text{dim},i}$ as a function of site i for electric field $\vec{E} = (0, 0, 4)$ and $\lambda_{D-}^{(0)} \neq 0$, where $r_L = \frac{L}{\pi} \sin(\frac{\pi x}{L})$. In (a,b,c), DMRG numerics are performed on a system of $L = 96$ sites using open boundary conditions, and in (d), DMRG numerics are performed on a system of $L = 96$ sites using periodic boundary condition. Bond dimension m and truncation error ϵ are chosen as $m = 1000$, $\epsilon = 10^{-10}$. The parameters of $K_1, J_1, \Gamma_1, \Gamma'_1, K_2, J_2$ in DMRG numerics are taken in accordance with Eq. (3) and Eq. (18).

As a result, the system remains in the Luttinger liquid phase.

2. Dimerization for $\lambda_{D-}^{(in)} \neq 0$

When $J_H \neq 0$, the $\lambda_{D-}^{(in)}$ term in Eq. (42) is nonvanishing, which changes sign under $R_1 I_2$ according to Eq. (23). Hence, the symmetry group $G'_{E,z}$ for $\lambda_{D-}^{(in)} \neq 0$ is

$$G'_{E,z} = \langle T, R_a^{-1} T_{2a} \rangle. \quad (45)$$

In this case, compared with the symmetry analysis in Sec. V B 1, the couplings ϵ , $(J''_L^z - J''_R^z)\epsilon$, $(J''_L^x + J''_R^x)N''_y - (J''_L^y + J''_R^y)N''_x$, and $J''_L^x J''_R^y - J''_L^y J''_R^x$ are no longer forbidden.

Since ϵ has the smallest scaling dimension (equal to 1/2) among all the symmetry allowed couplings, we only keep ϵ as the leading relevant perturbations, such that the low energy Hamiltonian $H_{E,z}^{\text{Low}}$ can be simplified as

$$H_{E,z}^{\text{Low}} = \int dx \left[\frac{2\pi v_3}{3} (\vec{J}'_L \cdot \vec{J}'_L + \vec{J}'_R \cdot \vec{J}'_R) + a_3 \epsilon \right]. \quad (46)$$

The effect of the relevant perturbation $\epsilon = \text{tr}(g)$ is to induce a dimerization in the ground states. The dimerization order parameter $O'_{\text{dim},i}$ in the six-sublattice rotated frame can be chosen as

$$O'_{\text{dim},i} = \vec{S}'_{i-1} \cdot \vec{S}'_i - \vec{S}'_i \cdot \vec{S}'_{i+1}, \quad (47)$$

and the expectation is that the ground state expectation value of $O'_{\text{dim},i}$ is nonvanishing as long as $\lambda_{D-}^{(in)}$ is nonzero.

3. Numerical results

For $\lambda_{D-}^{(0)} = 0$, as shown in Fig. 5 (a,b), we have calculated the staggered energy density $E_A(r)$ and entanglement entropy $S_L(x)$ with electric field $\vec{E}_{001} = (0, 0, 4)$ using DMRG calculations on systems of $L = 96$ sites under open boundary conditions, with parameters $K_1, J_1, \Gamma_1, \Gamma'_1, K_2, J_2$ and $\lambda_{D+}^{(\text{in})}, \lambda_D^{(\text{out})}, \lambda_\Gamma^{(\text{out})}$ chosen in accordance with Eq. (3) and Eq. (18). As can be seen from Fig. 5 (a,b), the DMRG numerical results are in good agreement with Luttinger liquid behaviors, giving a Luttinger parameter $\kappa = 0.9184$.

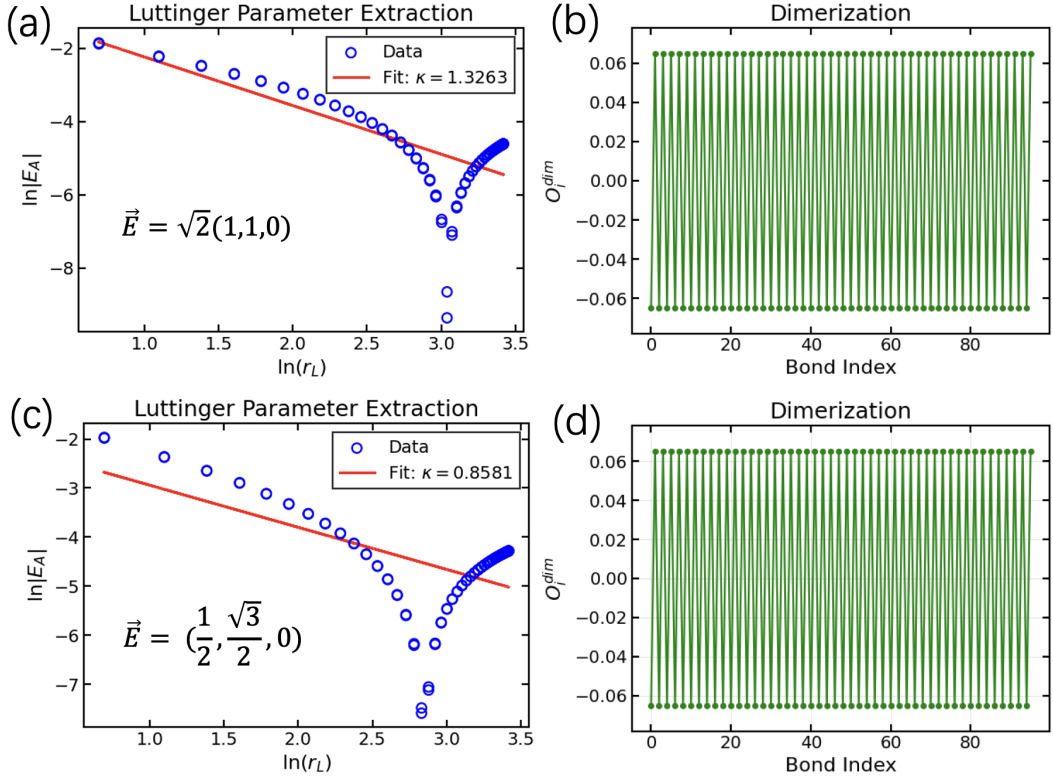


FIG. 6: (a,c) Staggered energy density $E_A(r)$ as a function of r_L on a log-log scale and (b,d) dimerization $O'_\text{dim,i}$ as a function of site i , with electric field $\vec{E} = \sqrt{2}(1,1,0)$ for (a,b) and $\vec{E} = (\frac{1}{2}, \frac{\sqrt{3}}{2}, 0)$ for (c,d), where $r_L = \frac{L}{\pi} \sin(\frac{\pi x}{L})$. In (a,b,c,d), DMRG numerics are performed on a system of $L = 96$ sites using open boundary conditions. Bond dimension m and truncation error ϵ chosen as $m = 1000$, $\epsilon = 10^{-10}$. The parameters of $K_1, J_1, \Gamma_1, \Gamma'_1, K_2, J_2$ in DMRG numerics are taken in accordance with Eq. (3) and Eq. (18).

For $\lambda_{D-}^{(0)} \neq 0$, we have calculated the staggered energy density $E_A(r)$ and dimerization $O'_\text{dim,i}$ for $\vec{E}_{001} = (0, 0, 4)$. $E_A(r)$ vs. r_L on a log-log scale and $O'_\text{dim,i}$ vs. site i are shown in Fig. 5 (c) and Fig. 5 (d), respectively. DMRG calculations are performed on a system of $L = 96$ sites under open boundary condition for $E_A(r)$ and periodic boundary condition for $O'_\text{dim,i}$, with parameters $K_1, J_1, \Gamma_1, \Gamma'_1, K_2, J_2$ and $\lambda_{D+}^{(\text{in})}, \lambda_{D-}^{(\text{in})}, \lambda_D^{(\text{out})}, \lambda_\Gamma^{(\text{out})}$ chosen in accordance with Eq. (3) and Eq. (18). As can be seen from Fig. 5 (c,d), no reliable Luttinger parameter can be extracted and the system has a nonzero dimerization. The DMRG numerical results are in good agreement with a non-Luttinger-liquid behavior.

C. Electric field along $(1, 1, 0)$ -direction

Next, we consider an electric field along $(1, 1, 0)$ -direction, as

$$\vec{E}_{110} = \frac{1}{\sqrt{2}} E_{110} (\hat{x} + \hat{y}). \quad (48)$$

Using Eq. (34), the Hamiltonian $H'_{E,110}$ in the U_6 frame can be obtained as

$$\begin{aligned} H'_{E,110} = & H' + \frac{1}{\sqrt{2}} E_{110} [\lambda_{D+}^{(\text{in})} (\mathcal{H}_{D,\text{odd}}^{(\text{in})} + \mathcal{H}_{D,\text{even}}^{(\text{in})}) \\ & + \lambda_{D-}^{(\text{in})} (\mathcal{H}_{D,\text{odd}}^{(\text{in})} - \mathcal{H}_{D,\text{even}}^{(\text{in})}) + \lambda_D^{(\text{out})} (\mathcal{H}_{D,\text{odd}}^{(\text{out})} + \mathcal{H}_{D,\text{even}}^{(\text{out})}) \\ & + \lambda_\Gamma^{(\text{out})} (\mathcal{H}_{\Gamma,\text{odd}}^{(\text{out})} + \mathcal{H}_{\Gamma,\text{even}}^{(\text{out})})], \end{aligned} \quad (49)$$

where H' is given in Eq. (8).

1. Dimerization

Since the $\lambda_{D-}^{(\text{in})}$ term in Eq. (49) changes sign under $R_I R_2$, the symmetry group $G'_{E,110}$ of $H'_{E,110}$ in the U_6 frame is

$$G'_{E,110} = \langle T, R_a^{-1} T_{2a} \rangle. \quad (50)$$

Based on a symmetry analysis, the low energy field theory is the same as Sec. V B 2, since the symmetry groups are the same. In particular, keeping only the most relevant coupling, the low energy Hamiltonian can be written as

$$H_{E,xy}^{\text{Low}} = \int dx \left[\frac{2\pi v_4}{3} (\vec{J}'_L \cdot \vec{J}'_L + \vec{J}'_R \cdot \vec{J}'_R) + a_4 \epsilon \right], \quad (51)$$

which has the same form as Eq. (46), but with different values of velocity v_4 and coupling constant a_4 . As a result, it is expected the system is in a dimerized phase.

2. Numerical results

We have calculated the staggered energy density $E_A(r)$ and dimerization $O'_{\text{dim},i}$ for $\vec{E}_{110} = \sqrt{2}(1, 1, 0)$. $E_A(r)$ vs. on a log-log scale and $O'_{\text{dim},i}$ vs. site i are shown in Fig. 6 (a) and Fig. 6 (b), respectively. DMRG calculations are performed on a system of $L = 96$ sites under open boundary condition for $E_A(r)$ and periodic boundary condition for $O'_{\text{dim},i}$, with parameters $K_1, J_1, \Gamma_1, \Gamma'_1, K_2, J_2$ and $\lambda_{D+}^{(\text{in})}, \lambda_{D-}^{(\text{in})}, \lambda_D^{(\text{out})}, \lambda_{\Gamma}^{(\text{out})}$ chosen in accordance with Eq. (3) and Eq. (18). As can be seen from Fig. 6 (a,b), no reliable Luttinger parameter can be extracted, and the system has a nonzero dimerization. The DMRG numerical results are in good agreement with a non-Luttinger-liquid behavior.

D. General electric fields

1. Dimerization

For electric fields along general directions, the r_2 and r_4 terms in Eq. (34) do not vanish, since the only case for both $r_2 = 0$ and $r_4 = 0$ is $E_x = E_y = E_z$ (namely, an electric field along $(1, 1, 1)$ -direction), as can be checked from the expressions for r_i ($1 \leq i \leq 4$) in Eq. (35). This means that for general electric fields, the system is not invariant under $R_I I_2$, and as a result, the dimerization operator ϵ is allowed in the low energy theory. Hence, the system is dimerized for generic electric fields.

2. Numerical results

We have calculated the staggered energy density $E_A(r)$ and dimerization $O'_{\text{dim},i}$ for $\vec{E}_{110} = (\frac{1}{2}, \frac{\sqrt{3}}{2}, 0)$. $E_A(r)$ vs.

on a log-log scale and $O'_{\text{dim},i}$ vs. site i are shown in Fig. 6 (c) and Fig. 6 (d), respectively. DMRG calculations are performed on a system of $L = 96$ sites under open boundary condition for $E_A(r)$ and periodic boundary condition for $O'_{\text{dim},i}$, with parameters $K_1, J_1, \Gamma_1, \Gamma'_1, K_2, J_2$ and $\lambda_{D+}^{(\text{in})}, \lambda_{D-}^{(\text{in})}, \lambda_D^{(\text{out})}, \lambda_{\Gamma}^{(\text{out})}$ chosen in accordance with Eq. (3) and Eq. (18). As can be seen from Fig. 6 (c,d), no reliable Luttinger parameter can be extracted, and the system has a nonzero dimerization. The DMRG numerical results are in good agreement with a non-Luttinger-liquid behavior.

VI. SUMMARY

In summary, we have studied effects of electric fields in the one-dimensional spin-1/2 $K_1 J_1 \Gamma_1 \Gamma'_1 K_2 J_2$ model in the parameter region $K_1 < 0, \Gamma_1 > 0, J > 0$, which is relevant for iridate materials. While the system is in a Luttinger liquid phase for zero electric field, we find that electric fields in general induce nonzero dimerization into the system, except that the electric field along $(1, 1, 1)$ -direction maintains the Luttinger liquid behavior. Our work builds a systematic understanding for electric field effects in generalized Kitaev spin-1/2 chains in the $K_1 < 0, \Gamma_1 > 0, J > 0$ region, and provides a starting point for approaching the 2D limit by considering a quasi-1D system of weakly coupled chains.

Acknowledgments

W.Y. and H.W. are supported by the National Natural Science Foundation of China (Grants No. 12474476) and the Fundamental Research Funds for the Central Universities. C.X. acknowledges the supports from MOST grant No. 2022YFA1403900, NSFC No. 12104451, NSFC No. 11920101005, and funds from Strategic Priority Research Program of CAS No. XDB28000000. The DMRG calculations in this work were performed using the software package ITensor in Ref. 91.

Appendix A: Electric field induced couplings

1. Expressions of couplings induced by electric fields

As derived in details in Ref. 84, $\lambda_{D+}^{(\text{in})}, \lambda_{D-}^{(\text{in})}, \lambda_D^{(\text{out})}, \lambda_\Gamma^{(\text{out})}$ in Eq. (15,17) are given by

$$\begin{aligned}\lambda_{D+}^{(\text{in})} &= -\frac{4IJ_F}{t} \frac{U_d - U_p + \Delta_{dp}}{2(U_d - U_p) + J_H} \\ \lambda_{D-}^{(\text{in})} &= -\frac{4IJ_F}{t} \frac{J_H}{2(U_d - U_p) + J_H} \\ \lambda_D^{(\text{out})} &= \frac{16t^3}{3} I \frac{1}{(U_d - U_p + \Delta_{dp})^2} \cdot \frac{J_H}{4(U_d - U_p + \Delta_{dp})^2 - J_H^2}, \\ \lambda_\Gamma^{(\text{out})} &= \frac{32t^3}{9} I \frac{1}{(U_d - U_p + \Delta_{dp})^2} \cdot \frac{U_d - U_p + \Delta_{dp}}{4(U_d - U_p + \Delta_{dp})^2 - J_H^2},\end{aligned}\quad (\text{A1})$$

in which t is the hopping integral between d - and p -orbitals; U_d and U_p are the strengths of on-site Hubbard interaction on d - and p -orbitals, respectively; J_H is the Hund's coupling at p -orbitals; Δ_{dp} is the orbital energy difference between d - and p -orbitals; I is the matrix element of the electric dipole moment between d - and p -orbitals; and J_F is given by

$$J_F = -\frac{8}{3}t^4 \frac{1}{2(U_d - U_p + \Delta_{dp})^2[(U_d - U_p + \Delta_{dp}) - J_H]}. \quad (\text{A2})$$

2. Estimations of magnitudes of couplings

In this appendix, we estimate the magnitudes of various coupling constants. We will not be very careful about the precise values of the couplings, but only focusing on their order of magnitudes.

In iridates, the microscopic parameters in Appendix A 1 are given by

$$U_d = 1.5\text{-}2.5\text{eV}, \quad U_p = 4\text{-}6\text{eV}, \quad J_H = 0.3\text{-}0.6\text{eV}, \quad t = 0.2\text{-}0.3\text{eV}, \quad \Delta_{dp} = 2\text{-}3\text{eV}, \quad I = 0.5\text{\AA}. \quad (\text{A3})$$

Plugging Eq. (A3) into Eqs. (A1,A2), we obtain

$$\begin{aligned}\lambda_{D+}^{(\text{in})} I &= -1.51 \times 10^{-3} \text{nm} \\ \lambda_{D-}^{(\text{in})} I &= -0.76 \times 10^{-3} \text{nm} \\ \lambda_D^{(\text{out})} I &= 0.55 \times 10^{-3} \text{nm} \\ \lambda_\Gamma^{(\text{out})} I &= 0.74 \times 10^{-3} \text{nm}.\end{aligned}\quad (\text{A4})$$

Measuring electric fields in unit of eV/nm, the parameters in Eq. (A4) can be written as

$$\begin{aligned}\lambda_{D+}^{(\text{in})} I &\rightarrow -1.51 \text{meV} \\ \lambda_{D-}^{(\text{in})} I &\rightarrow -0.76 \text{meV} \\ \lambda_D^{(\text{out})} I &\rightarrow 0.55 \text{meV} \\ \lambda_\Gamma^{(\text{out})} I &\rightarrow 0.74 \text{meV}.\end{aligned}\quad (\text{A5})$$

On the other hand, the values of $K_1, J_1, \Gamma_1, \Gamma'_1, K_2, J_2$ are

$$-K_1 = 10\text{-}25\text{meV}, \quad J_1 = 1\text{-}5\text{meV}, \quad \Gamma_1 = 5\text{-}15\text{meV}, \quad \Gamma'_1 = 0.5\text{-}3\text{meV}, \quad K_2 = 0\text{-}1\text{meV}, \quad J_2 = 1\text{-}5\text{meV}. \quad (\text{A6})$$

Normalizing $K_1^2 + J_1^2 + \Gamma_1^2 = 1$, a typical realistic set of parameters can be chosen as

$$\theta = 0.44\pi, \quad \phi = 0.85\pi, \quad (\text{A7})$$

and

$$\Gamma' = 0.1, \quad K_2 = 0.02, \quad J_2 = 0.2, \quad \lambda_{D+}^{(\text{in})} = -0.1, \quad \lambda_{D-}^{(\text{in})} = -0.05, \quad \lambda_D^{(\text{out})} = 0.04, \quad \lambda_\Gamma^{(\text{out})} = 0.05, \quad (\text{A8})$$

in which θ, ϕ are defined in Eq. (2), and the unit is on the order of 10meV.

Appendix B: Explicit forms of the Hamiltonians

In this appendix, we include the explicit forms of various terms in the Hamiltonian in both unrotated and six-sublattice rotated frames.

1. Hamiltonians in unrotated frame

Since the Hamiltonian has a two-site periodicity, we only present the terms within the first unit cell which contains two bonds.

a. $K_1 J_1 \Gamma_1 \Gamma'_1 K_2 J_2$ model

1. $KS_1^x S_2^x + J(S_1^x S_2^x + S_1^y S_2^y + S_1^z S_2^z) + \Gamma(S_1^y S_2^z + S_1^z S_2^y) + \Gamma'(S_1^x S_2^y + S_1^y S_2^x + S_1^z S_2^z + S_1^z S_2^x) + K_2 S_2^z S_3^z + J_2(S_1^x S_3^x + S_1^y S_3^y + S_1^z S_3^z)$
2. $KS_2^y S_3^y + J(S_2^x S_3^x + S_2^y S_3^y + S_2^z S_3^z) + \Gamma(S_2^z S_3^x + S_2^x S_3^z) + \Gamma'(S_2^y S_3^z + S_2^z S_3^y + S_2^y S_3^x + S_2^x S_3^y) + K_2 S_2^z S_4^z + J_2(S_2^x S_4^x + S_2^y S_4^y + S_2^z S_4^z)$. (B1)

b. Electric fields

The terms induced by an electric field along x -direction are given by

1. $E_x [\lambda_D^{(\text{out})} (S_1^z S_2^x - S_1^x S_2^z + S_1^x S_2^y - S_1^y S_2^x) + \lambda_\Gamma^{(\text{out})} (S_1^x S_2^y + S_1^y S_2^x + S_1^z S_2^z + S_1^z S_2^x)]$
2. $E_x (\lambda_{D+}^{(\text{in})} - \lambda_{D-}^{(\text{in})}) (S_2^z S_3^x - S_2^x S_3^z)$. (B2)

The terms induced by an electric field along y -direction are given by

1. $(\lambda_{D+}^{(\text{in})} + \lambda_{D-}^{(\text{in})}) E_y (S_1^y S_2^z - S_1^z S_2^y)$
2. $\lambda_D^{(\text{out})} E_y (S_2^x S_3^y - S_2^y S_3^x + S_2^y S_3^z - S_2^z S_3^y) + \lambda_\Gamma^{(\text{out})} E_y (S_2^y S_3^z + S_2^z S_3^y + S_2^y S_3^x + S_2^x S_3^y)$. (B3)

The terms induced by an electric field along z -direction are given by

1. $(\lambda_{D+}^{(\text{in})} - \lambda_{D-}^{(\text{in})}) E_z (S_1^y S_2^z - S_1^z S_2^y)$
2. $(\lambda_{D+}^{(\text{in})} + \lambda_{D-}^{(\text{in})}) E_z (S_2^z S_3^x - S_2^x S_3^z)$. (B4)

2. Hamiltonians in six-sublattice rotated frame

Since the Hamiltonian has a six-site periodicity, we only present the terms within the first unit cell which contains six bonds. The $K_1 J_1 \Gamma_1 \Gamma'_1 K_2 J_2$ model is an exception, which is three-site periodic, so we only include the first three bonds for this model.

a. $K_1 J_1 \Gamma_1 \Gamma'_1 K_2 J_2$ model

1. $-KS'_1 S'^x_2 - J(S'_1 S'^x_2 + S'_1 S'^y_2 + S'_1 S'^z_2 + S'_1 S'^y_2) + \Gamma(S'_1 S'^y_2 + S'_1 S'^z_2) + \Gamma'(-S'_1 S'^z_2 - S'_1 S'^y_2 + S'_1 S'^x_2 + S'_1 S'^z_2)$
 $+K_2 S'_1 S'^x_3 + J_2(S'_1 S'^y_3 + S'_1 S'^z_3 + S'_1 S'^x_3)$
2. $-KS'_2 S'^z_3 - J(S'_2 S'^y_3 + S'_2 S'^z_3 + S'_2 S'^x_3) + \Gamma(S'_2 S'^y_3 + S'_2 S'^x_3) + \Gamma'(S'_2 S'^x_3 + S'_2 S'^z_3 - S'_2 S'^y_3 - S'_2 S'^z_3)$
 $+K_2 S'_2 S'^z_4 + J_2(S'_2 S'^y_4 + S'_2 S'^z_4 + S'_2 S'^x_4)$
3. $-KS'_3 S'^y_4 - J(S'_3 S'^y_4 + S'_3 S'^z_4 + S'_3 S'^x_4) + \Gamma(S'_3 S'^z_4 + S'_3 S'^x_4) + \Gamma'(-S'_3 S'^x_4 - S'_3 S'^y_4 + S'_3 S'^z_4 + S'_3 S'^y_4)$
 $+K_2 S'_3 S'^y_5 + J_2(S'_3 S'^z_5 + S'_3 S'^x_5 + S'_3 S'^y_5)$

b. Electric fields

The terms induced by an electric field along x -direction are given by

1. $E_x \left[\lambda_D^{(\text{out})} (S'_1 S'^x_2 - S'_1 S'^y_2 - S'_1 S'^z_2 + S'_1 S'^x_2) + \lambda_\Gamma^{(\text{out})} (-S'_1 S'^z_2 - S'_1 S'^y_2 + S'_1 S'^x_2 + S'_1 S'^z_2) \right]$
2. $E_x \left(\lambda_{D+}^{(\text{in})} - \lambda_{D-}^{(\text{in})} \right) (S'_2 S'^y_3 - S'_2 S'^x_3)$
3. $E_x \left[\lambda_D^{(\text{out})} (S'_3 S'^y_4 - S'_3 S'^z_4 - S'_3 S'^x_4 + S'_3 S'^y_4) + \lambda_\Gamma^{(\text{out})} (-S'_3 S'^x_4 - S'_3 S'^y_4 + S'_3 S'^z_4 + S'_3 S'^x_4) \right]$
4. $E_x \left(\lambda_{D+}^{(\text{in})} - \lambda_{D-}^{(\text{in})} \right) (S'_4 S'^z_5 - S'_4 S'^y_5)$
5. $E_x \left[\lambda_D^{(\text{out})} (S'_5 S'^z_6 - S'_5 S'^x_6 - S'_5 S'^y_6 + S'_5 S'^z_6) + \lambda_\Gamma^{(\text{out})} (-S'_5 S'^y_6 - S'_5 S'^z_6 + S'_5 S'^x_6 + S'_5 S'^y_6) \right]$
6. $E_x \left(\lambda_{D+}^{(\text{in})} - \lambda_{D-}^{(\text{in})} \right) (S'_6 S'^x_7 - S'_6 S'^z_7)$

(B6)

The terms induced by an electric field along y -direction are given by

1. $E_y (\lambda_{D+}^{(\text{in})} + \lambda_{D-}^{(\text{in})}) (S'_1 S'^y_2 - S'_1 S'^z_2)$
2. $E_y \left[\lambda_D^{(\text{out})} (-S'_2 S'^z_3 + S'_2 S'^y_3 + S'_2 S'^x_3 - S'_2 S'^z_3) + \lambda_\Gamma^{(\text{out})} (S'_2 S'^x_3 + S'_2 S'^z_3 - S'_2 S'^y_3 - S'_2 S'^x_3) \right]$
3. $E_y (\lambda_{D+}^{(\text{in})} + \lambda_{D-}^{(\text{in})}) (S'_3 S'^z_4 - S'_3 S'^x_4)$
4. $E_y \left[\lambda_D^{(\text{out})} (-S'_4 S'^x_5 + S'_4 S'^z_5 + S'_4 S'^y_5 - S'_4 S'^x_5) + \lambda_\Gamma^{(\text{out})} (S'_4 S'^y_5 + S'_4 S'^x_5 - S'_4 S'^z_5 - S'_4 S'^x_5) \right]$
5. $E_y (\lambda_{D+}^{(\text{in})} + \lambda_{D-}^{(\text{in})}) (S'_5 S'^x_6 - S'_5 S'^y_6)$
6. $E_y \left[\lambda_D^{(\text{out})} (-S'_6 S'^y_7 + S'_6 S'^x_7 + S'_6 S'^z_7 - S'_6 S'^y_7) + \lambda_\Gamma^{(\text{out})} (S'_6 S'^z_7 + S'_6 S'^y_7 - S'_6 S'^x_7 - S'_6 S'^z_7) \right].$

The terms induced by an electric field along z -direction are given by

1. $E_z (\lambda_{D+}^{(\text{in})} - \lambda_{D-}^{(\text{in})}) (S'_1 S'^y_2 - S'_1 S'^z_2)$
2. $E_z (\lambda_{D+}^{(\text{in})} + \lambda_{D-}^{(\text{in})}) (S'_2 S'^y_3 - S'_2 S'^x_3)$
3. $E_z (\lambda_{D+}^{(\text{in})} - \lambda_{D-}^{(\text{in})}) (S'_3 S'^z_4 - S'_3 S'^x_4)$
4. $E_z (\lambda_{D+}^{(\text{in})} + \lambda_{D-}^{(\text{in})}) (S'_4 S'^z_5 - S'_4 S'^y_5)$
5. $E_z (\lambda_{D+}^{(\text{in})} - \lambda_{D-}^{(\text{in})}) (S'_5 S'^x_6 - S'_5 S'^y_6)$
6. $E_z (\lambda_{D+}^{(\text{in})} + \lambda_{D-}^{(\text{in})}) (S'_6 S'^x_7 - S'_6 S'^z_7).$

(B8)

Appendix C: Symmetry transformation properties of electric field terms

It is easier to analyze the transformations in the unrotated frame, since the periodicity of the bond pattern is shorter (i.e., two in the unrotated frame rather than six in the U_6 frame).

According to Eq. (13), G' in Eq. (12) can be written as

$$\begin{aligned} G' &= U_6 G U_6^{-1} \\ &= U_6 \langle T, R(\hat{n}_N, \pi) T_a, R(\hat{n}_N, \pi) I_0 \rangle U_6^{-1}. \end{aligned} \quad (C1)$$

As a result, for the purpose of knowing how electric field terms transform under $T, R_a T_a, R_I I_2$ in the U_6 frame, it is enough to work out how they transform under $T, R(\hat{n}_N, \pi) T_a, R(\hat{n}_N, \pi) I_0$ in the unrotated frame. Apparently, any uniform electric field is invariant under T and T_{2a} . We will consider how they transform under $R(\hat{n}_N, \pi) I_0$ and $R(\hat{n}_N, \pi) T_a$.

We introduce the following terms in the unrotated frame,

$$\begin{aligned} \mathcal{H}_{D, \text{odd/even}}^{(\text{in})} &= \sum_{\substack{\langle ij \rangle \in \gamma \text{ bond} \\ i \in \text{odd/even}}} (S_i^\alpha S_{i+1}^\beta - S_i^\beta S_{i+1}^\alpha) \\ \mathcal{H}_{D, \text{odd/even}}^{(\text{out})} &= \sum_{\substack{\langle ij \rangle \in \gamma \text{ bond} \\ i \in \text{odd/even}}} (S_i^\beta S_{i+1}^\gamma - S_i^\gamma S_{i+1}^\beta + S_i^\gamma S_{i+1}^\alpha - S_i^\alpha S_{i+1}^\gamma) \\ \mathcal{H}_{\Gamma, \text{odd/even}}^{(\text{out})} &= \sum_{\substack{\langle ij \rangle \in \gamma \text{ bond} \\ i \in \text{odd/even}}} (S_i^\gamma S_{i+1}^\alpha + S_i^\alpha S_{i+1}^\gamma + S_i^\gamma S_{i+1}^\beta + S_i^\beta S_{i+1}^\gamma). \end{aligned} \quad (C2)$$

It can be verified that the couplings in Eq. (C2) transform as

$$\begin{aligned} R(\hat{n}_N, \pi) T_a : \mathcal{H}_{D, \text{odd}}^{(\text{in})} &\longleftrightarrow -\mathcal{H}_{D, \text{even}}^{(\text{in})} \\ \mathcal{H}_{D, \text{odd}}^{(\text{out})} &\longleftrightarrow -\mathcal{H}_{D, \text{even}}^{(\text{out})} \\ \mathcal{H}_{\Gamma, \text{odd}}^{(\text{out})} &\longleftrightarrow \mathcal{H}_{\Gamma, \text{even}}^{(\text{out})}, \end{aligned} \quad (C3)$$

and

$$\begin{aligned} R(\hat{n}_N, \pi) I_0 : \mathcal{H}_{D, \text{odd}}^{(\text{in})} &\longleftrightarrow \mathcal{H}_{D, \text{even}}^{(\text{in})} \\ \mathcal{H}_{D, \text{odd}}^{(\text{out})} &\longleftrightarrow \mathcal{H}_{D, \text{even}}^{(\text{out})} \\ \mathcal{H}_{\Gamma, \text{odd}}^{(\text{out})} &\longleftrightarrow \mathcal{H}_{\Gamma, \text{even}}^{(\text{out})}. \end{aligned} \quad (C4)$$

Denote

$$\begin{aligned} \mathcal{H}'_{D, \text{odd/even}}^{(\text{in})} &= U_6 \mathcal{H}_{D, \text{odd/even}}^{(\text{in})} U_6^{-1}, \\ \mathcal{H}'_{D, \text{odd/even}}^{(\text{out})} &= U_6 \mathcal{H}_{D, \text{odd/even}}^{(\text{out})} U_6^{-1}, \\ \mathcal{H}'_{\Gamma, \text{odd/even}}^{(\text{out})} &= U_6 \mathcal{H}_{\Gamma, \text{odd/even}}^{(\text{out})} U_6^{-1}, \end{aligned} \quad (C5)$$

which are exactly Eq. (21). Explicit forms of the terms in Eq. (C5) in the U_6 frame are included in Appendix B. All terms in Eq. (C5) are all invariant under $U_6 T U_6^{-1} = T$ and $U_6 T_{2a} U_6^{-1} = R_a^{-1} T_{2a}$. Furthermore, their transformation properties under $R_a T_a$ and $R_I I_2$ can be obtained from Eqs. (C3,C4) as Eqs. (22,23).

Appendix D: Transformation rules of WZW fields

The transformation properties of the WZW fields g and \vec{J}'_L, \vec{J}'_R under time reversal T , spatial translation T_a , spatial inversion I with inversion center located at sites, and global spin rotation $R \in SO(3)$ are given by

$$\begin{aligned} T : \quad \epsilon(x) &\rightarrow \epsilon(x), \quad \vec{N}'(x) \rightarrow -\vec{N}'(x), \\ \vec{J}'_L(x) &\rightarrow -\vec{J}'_R(x), \quad \vec{J}'_R(x) \rightarrow -\vec{J}'_L(x), \end{aligned} \quad (D1)$$

$$T_a : \begin{aligned} \epsilon(x) &\rightarrow -\epsilon(x), & \vec{N}'(x) &\rightarrow -\vec{N}'(x), \\ \vec{J}'_L(x) &\rightarrow \vec{J}'_L(x), & \vec{J}'_R(x) &\rightarrow \vec{J}'_R(x), \end{aligned} \quad (D2)$$

$$I : \begin{aligned} \epsilon(x) &\rightarrow -\epsilon(-x), & \vec{N}'(x) &\rightarrow \vec{N}'(-x), \\ \vec{J}'_L(x) &\rightarrow \vec{J}'_R(-x), & \vec{J}'_R(x) &\rightarrow \vec{J}'_L(-x), \end{aligned} \quad (D3)$$

$$R : \begin{aligned} \epsilon(x) &\rightarrow \epsilon(x), & N'^\alpha(x) &\rightarrow R_\beta^\alpha N'^\beta(x), \\ J'^\alpha_L(x) &\rightarrow R_\beta^\alpha J'^\beta_L(x), & J'^\alpha_R(x) &\rightarrow R_\beta^\alpha J'^\beta_R(x). \end{aligned} \quad (D4)$$

in which x is the spatial coordinate; R_β^α ($\alpha, \beta = x, y, z$) is the matrix element of the 3×3 rotation matrix R at position (α, β) .

¹ G. Jackeli and G. Khaliullin, *Mott Insulators in the Strong Spin-Orbit Coupling Limit: From Heisenberg to a Quantum Compass and Kitaev Models*, Phys. Rev. Lett. **102**, 017205 (2009).

² J. Chaloupka, G. Jackeli, and G. Khaliullin, *Kitaev-Heisenberg Model on a Honeycomb Lattice: Possible Exotic Phases in Iridium Oxides A_2IrO_3* , Phys. Rev. Lett. **105**, 027204 (2010).

³ Y. Singh and P. Gegenwart, *Antiferromagnetic Mott insulating state in single crystals of the honeycomb lattice material Na_2IrO_3* , Phys. Rev. B **82**, 064412 (2010).

⁴ C. C. Price and N. B. Perkins, *Critical Properties of the Kitaev-Heisenberg Model*, Phys. Rev. Lett. **109**, 187201 (2012).

⁵ Y. Singh, S. Manni, J. Reuther, T. Berlijn, R. Thomale, W. Ku, S. Trebst, and P. Gegenwart, *Relevance of the Heisenberg-Kitaev Model for the Honeycomb Lattice Iridates A_2IrO_3* , Phys. Rev. Lett. **108**, 127203 (2012).

⁶ K. W. Plumb, J. P. Clancy, L. J. Sandilands, V. V. Shankar, Y. F. Hu, K. S. Burch, H. Y. Kee, and Y. J. Kim, *α -RuCl₃: A spin-orbit assisted Mott insulator on a honeycomb lattice*, Phys. Rev. B **90**, 041112(R) (2014).

⁷ H.-S. Kim, V. S. V., A. Catuneanu, and H.-Y. Kee, *Kitaev magnetism in honeycomb RuCl₃ with intermediate spin-orbit coupling*, Phys. Rev. B **91**, 241110(R) (2015).

⁸ S. M. Winter, Y. Li, H. O. Jeschke, and R. Valentí, *Challenges in design of Kitaev materials: Magnetic interactions from competing energy scales*, Phys. Rev. B **93**, 214431 (2016).

⁹ S. H. Baek, S. H. Do, K. Y. Choi, Y. Kwon, A. Wolter, S. Nishimoto, J. van den Brink, and B. Buchner, *Evidence for a Field-Induced Quantum Spin Liquid in α -RuCl₃*, Phys. Rev. Lett. **119**, 037201 (2017).

¹⁰ I. A. Leahy, C. A. Pocs, P. E. Siegfried, D. Graf, S. H. Do, K. Y. Choi, B. Normand, and M. Lee, *Anomalous Thermal Conductivity and Magnetic Torque Response in the Honeycomb Magnet α -RuCl₃*, Phys. Rev. Lett. **118**, 187203 (2017).

¹¹ J. A. Sears, Y. Zhao, Z. Xu, J. W. Lynn, and Y. J. Kim, *Phase diagram of α -RuCl₃ in an in-plane magnetic field*, Phys. Rev. B **95**, 180411(R) (2017).

¹² A. U. B. Wolter, L. T. Corredor, L. Janssen, K. Nenkov, S. Schonecker, S. H. Do, K. Y. Choi, R. Albrecht, J. Hunger, T. Doert, M. Vojta, and B. Buchner, *Field-induced quantum criticality in the Kitaev system α -RuCl₃*, Phys. Rev. B **96**, 041405(R) (2017).

¹³ J. Zheng, K. Ran, T. Li, J. Wang, P. Wang, B. Liu, Z.-X. Liu, B. Normand, J. Wen, and W. Yu, *Gapless Spin Excitations in the Field-Induced Quantum Spin Liquid Phase of α -RuCl₃*, Phys. Rev. Lett. **119**, 227208 (2017).

¹⁴ I. Roussochatzakis and N. B. Perkins, *Classical Spin Liquid Instability Driven By Off-Diagonal Exchange in Strong Spin-Orbit Magnets*, Phys. Rev. Lett. **118**, 147204 (2017).

¹⁵ Y. Kasahara, T. Ohnishi, N. Kurita, H. Tanaka, J. Nasu, Y. Motome, T. Shibauchi, and Y. Matsuda, *Majorana quantization and half-integer thermal quantum Hall effect in a Kitaev spin liquid*, Nature (London) **559**, 227 (2018).

¹⁶ J. G. Rau, E. K. H. Lee, and H. Y. Kee, *Generic Spin Model for the Honeycomb Iridates beyond the Kitaev Limit*, Phys. Rev. Lett. **112**, 077204 (2014).

¹⁷ K. Ran, J. Wang, W. Wang, Z.-Y. Dong, X. Ren, S. Bao, S. Li, Z. Ma, Y. Gan, Y. Zhang, J. T. Park, G. Deng, S. Danilkin, S.-L. Yu, J.-X. Li, and J. Wen, *Spin-Wave Excitations Evidencing the Kitaev Interaction in Single Crystalline α -RuCl₃*, Phys. Rev. Lett. **118**, 107203 (2017).

¹⁸ W. Wang, Z.-Y. Dong, S.-L. Yu, and J.-X. Li, *Theoretical investigation of magnetic dynamics in α -RuCl₃*, Phys. Rev. B **96**, 115103 (2017).

¹⁹ A. Catuneanu, Y. Yamaji, G. Wachtel, Y. B. Kim, and H.-Y. Kee, *Path to stable quantum spin liquids in spin-orbit coupled correlated materials*, npj Quantum Mater. **3**, 23 (2018).

²⁰ M. Gohlke, G. Wachtel, Y. Yamaji, F. Pollmann, and Y. B. Kim, *Quantum spin liquid signatures in Kitaev-like frustrated magnets*, Phys. Rev. B **97**, 075126 (2018).

²¹ X. Liu, T. Berlijn, W.-G. Yin, W. Ku, A. Tsvelik, Young-June Kim, H. Gretarsson, Yogesh Singh, P. Gegenwart, and J. P. Hill, *Long-range magnetic ordering in Na_2IrO_3* , Phys. Rev. B **83**, 220403(R) (2011).

²² J. Chaloupka, G. Jackeli, and G. Khaliullin, *Zigzag Magnetic Order in the Iridium Oxide Na_2IrO_3* , Phys. Rev. Lett. **110**, 097204 (2013).

²³ R. D. Johnson, S. C. Williams, A. A. Haghaghirad, J. Singleton, V. Zapf, P. Manuel, I. I. Mazin, Y. Li, H.

O. Jeschke, R. Valentí, and R. Coldea, *Monoclinic crystal structure of α -RuCl₃ and the zigzag antiferromagnetic ground state*, Phys. Rev. B **92**, 235119 (2015).

²⁴ Motome, R. Sano, S. H. Jang, Y. Sugita, and Y. Kato, *Materials design of Kitaev spin liquids beyond the Jackeli-Khaliullin mechanism*, J. Phys.: Condens. Matter **32**, 404001 (2020).

²⁵ A. Kitaev, *Anyons in an exactly solved model and beyond*, Ann. Phys. (N. Y.) **321**, 2 (2006).

²⁶ C. Nayak, S. H. Simon, A. Stern, M. Freedman, and S. Das Sarma, *Non-Abelian anyons and topological quantum computation*, Rev. Mod. Phys. **80**, 1083 (2008).

²⁷ M. Hermanns, I. Kimchi, and J. Knolle, *Physics of the Kitaev model: Fractionalization, dynamic correlations, and material connections*, Annu. Rev. Condens. Matter Phys. **9**, 17 (2018).

²⁸ H. Takagi, T. Takayama, G. Jackeli, G. Khaliullin, and S. E. Nagler, *Concept and realization of Kitaev quantum spin liquids*, Nat. Rev. Phys. **1**, 264 (2019).

²⁹ S. Trebst, *Kitaev materials*, Phys. Rep. **950**, 1 (2022).

³⁰ Y. Matsuda, T. Shibauchi, and H.-Y. Kee, Rev. Mod. Phys. **97**, 045003 (2025).

³¹ T. Yokoi, S. Ma, Y. Kasahara, S. Kasahara, T. Shibauchi, N. Kurita, H. Tanaka, J. Nasu, Y. Motome, C. Hickey, S. Trebst, and Y. Matsuda, *Half-integer quantized anomalous thermal Hall effect in the Kitaev material α -RuCl₃*, Science **373**, 568 (2021).

³² J. A. N. Bruin, R. R. K. Singh, M. S. Griffin, Y. Kasahara, N. Kurita, H. Tanaka, and Y. Matsuda, *Robustness of the thermal Hall effect close to half-quantization in α -RuCl₃*, Nat. Phys. **18**, 401 (2022).

³³ P. Czajka, T. Gao, M. McGuire, D. G. Mandrus, P. Lampen-Kelley, J.-Q. Yan, S. E. Nagler, and N. P. Butch, *Oscillations of the thermal conductivity in the spin-liquid state of α -RuCl₃*, Nat. Phys. **17**, 915 (2021).

³⁴ H. Liu, J. Chaloupka, and G. Khaliullin, *Exchange interactions in d^5 Kitaev materials: From Na₂IrO₃ to α -RuCl₃*, Phys. Rev. B **105**, 214411 (2022).

³⁵ F. D. M. Haldane, *Effective Harmonic-Fluid Approach to Low-Energy Properties of One-Dimensional Quantum Fluids*, J. Phys. C: Solid State Phys. **14**, 2585 (1981).

³⁶ F. D. M. Haldane, *Luttinger liquid theory of one-dimensional quantum fluids: I. Properties of the Luttinger model and their extension to the general 1D interacting spinless Fermi gas*, Phys. Rev. Lett. **47**, 1840 (1981).

³⁷ A. A. Belavin, A. M. Polyakov, and A. B. Zamolodchikov, *Infinite conformal symmetry in two-dimensional quantum field theory*, Nucl. Phys. B **241**, 333 (1984).

³⁸ V. G. Knizhnik and A. B. Zamolodchikov, *Current algebra and Wess-Zumino model in two dimensions*, Nucl. Phys. B **247**, 83 (1984).

³⁹ I. Affleck, *Critical behaviour of SU(n) quantum chains and topological non-linear sigma models*, Phys. Rev. Lett. **55**, 1355 (1985).

⁴⁰ I. Affleck, *Field theory methods and quantum critical phenomena*, in *Fields, Strings and Critical Phenomena*, Proceedings of the Les Houches Summer School, 1988, edited by E. Brézin and J. Zinn-Justin (North-Holland, Amsterdam, 1990), pp. 563–640.

⁴¹ I. Affleck, *Conformal field theory approach to the Kondo effect*, Acta Phys. Polon. B **26**, 1869 (1995).

⁴² S. R. White, *Density matrix formulation for quantum renormalization groups*, Phys. Rev. Lett. **69**, 2863 (1992).

⁴³ S. R. White, *Density-matrix algorithms for quantum renormalization groups*, Phys. Rev. B **48**, 10345 (1993).

⁴⁴ U. Schollwöck, *The density-matrix renormalization group in the age of matrix product states*, Ann. Phys. (N.Y.) **326**, 96 (2011).

⁴⁵ E. Sela, H.-C. Jiang, M. H. Gerlach, and S. Trebst, *Order-by-disorder and spin-orbital liquids in a distorted Heisenberg-Kitaev model*, Phys. Rev. B **90**, 035113 (2014).

⁴⁶ C. E. Agranidis, J. van den Brink, and S. Nishimoto, *Ordered states in the Kitaev-Heisenberg model: From 1D chains to 2D honeycomb*, Sci. Rep. **8**, 1815 (2018).

⁴⁷ C. E. Agranidis, J. van den Brink, and S. Nishimoto, *Ground state and low-energy excitations of the Kitaev-Heisenberg two-leg ladder*, Phys. Rev. B **99**, 224418 (2019).

⁴⁸ A. Catuneanu, E. S. Sørensen, and H.-Y. Kee, *Nonlocal string order parameter in the $S = 1/2$ Kitaev-Heisenberg ladder*, Phys. Rev. B **99**, 195112 (2019).

⁴⁹ W. Yang, A. Nocera, T. Tummmuru, H.-Y. Kee, and I. Affleck, *Phase Diagram of the Spin-1/2 Kitaev-Gamma Chain and Emergent SU(2) Symmetry*, Phys. Rev. Lett. **124**, 147205 (2020).

⁵⁰ W. Yang, A. Nocera, and I. Affleck, *Comprehensive study of the phase diagram of the spin-1/2 Kitaev-Heisenberg-Gamma chain*, Phys. Rev. Research **2**, 033268 (2020).

⁵¹ W. Yang, A. Nocera, and I. Affleck, *Spin wave theory of a one-dimensional generalized Kitaev model*, Phys. Rev. B **102**, 134419 (2020).

⁵² W. Yang, A. Nocera, E. S. Sørensen, H.-Y. Kee, and I. Affleck, *Classical spin order near the antiferromagnetic Kitaev point in the spin-1/2 Kitaev-Gamma chain*, Phys. Rev. B **103**, 054437 (2021).

⁵³ W. Yang, A. Nocera, P. Herringer, R. Raussendorf, I. Affleck, *Symmetry analysis of bond-alternating Kitaev spin chains and ladders*, Phys. Rev. B **105**, 094432 (2022).

⁵⁴ W. Yang, C. Xu, S. Xu, A. Nocera, I. Affleck, *Nonsymmorphic Luttinger liquids in generalized antiferromagnetic Kitaev spin-1/2 chains*, Phys. Rev. B **109**, L180403 (2024).

⁵⁵ W. Yang, C. Xu, A. Nocera, I. Affleck, *Origin of non-symmorphic bosonization formulas in generalized antiferromagnetic Kitaev spin-1/2 chains from a renormalization-group perspective*, Phys. Rev. B **106**, 064425 (2022).

⁵⁶ W. Yang, A. Nocera, C. Xu, S. Ma, A. Adhikary, and I. Affleck, *Emergent SU(2)₁ conformal symmetry in the spin-1/2 Kitaev-Gamma chain with a Dzyaloshinskii-Moriya interaction*, Phys. Rev. B **111**, 174414 (2025).

⁵⁷ W. Yang, C. Xu, S. Ma, A. Nocera, and I. Affleck, *Left-left-right-right magnetic order in spin-1/2 Kitaev-Heisenberg chain*, Phys. Rev. B, **112**, 035104 (2025).

⁵⁸ W. Yang, A. Nocera, C. Xu, and I. Affleck, *Nonsymmorphic spin-space cubic groups and SU(2)₁ conformal invariance in one-dimensional spin-1/2 models*, SciPost Phys. **17**, 097 (2024).

⁵⁹ Q. Luo, J. Zhao, X. Wang, and H.-Y. Kee, *Unveiling the phase diagram of a bond-alternating spin- $\frac{1}{2}$ K- Γ chain*, Phys. Rev. B **103**, 144423 (2021).

⁶⁰ Q. Luo, S. Hu, and H.-Y. Kee, *Unusual excitations and double-peak specific heat in a bond-alternating spin-1 chain*, Phys. Rev. Research **3**, 033048 (2021).

⁶¹ E. S. Sørensen, A. Catuneanu, J. Gordon, H.-Y. Kee, *Heart of Entanglement: Chiral, Nematic, and Incommensurate Phases in the Kitaev-Gamma Ladder in a Field*, Phys. Rev. X **11**, 011013 (2021).

⁶² Z.-A. Liu, T.-C. Yi, J.-H. Sun, Y.-L. Dong, and W.-L. You, *Lifshitz phase transitions in a one-dimensional Gamma model*, Phys. Rev. E **102**, 032127 (2020).

⁶³ Z.-A. Liu, Y.-L. Dong, N. Wu, Y. Wang, and W.-L. You, *Quantum criticality and correlations in the Ising-Gamma chain*, *Physica A* **579**, 126122 (2021).

⁶⁴ Z. Zhao, T.-C. Yi, M. Xue, and W.-L. You, *Characterizing quantum criticality and steered coherence in the XY-Gamma chain*, *Phys. Rev. A* **105**, 063306 (2022).

⁶⁵ S. Kheiri, H. Cheraghi, S. Mahdavifar, and N. Sedlmayr, *Information propagation in one-dimensional XY- Γ chains*, *Phys. Rev. B* **109**, 134303 (2024).

⁶⁶ S. Mahdavifar and D. C. Liu, *Anisotropic spin-1/2 XXZ chains with uniform gamma interaction*, *Sci. Rep.* **14**, 30024 (2024).

⁶⁷ M. Abbasi, S. Mahdavifar, and M. Motamedifar, *Spin-1/2 XX chains with modulated Gamma interaction*, *SciPost Phys. Core* **8**, 001 (2025).

⁶⁸ X. Jin, D. C. Liu, Y. Shi, A. M. Chen, and Y. H. Su, *Quantum phase transitions in the spin-1/2 XXZ model with staggered γ interaction*, *Phys. Rev. E* **111**, 014110 (2025).

⁶⁹ M. Abbasi, S. Mahdavifar, and M. Motamedifar, *Hybrid critical line in the spin-1/2 XX chain with gamma interaction under transverse fields*, *Sci. Rep.* **15**, 20469 (2025).

⁷⁰ M. Abbasi, S. Mahdavifar, and M. Motamedifar, *Concurrenceless and QDless line in the ground state phase diagram of the spin-1/2 XX chain with uniform gamma interaction*, *Results in Physics* **76**, 108362 (2025).

⁷¹ H. Saito and C. Hotta, *Exact matrix product states at the quantum Lifshitz tricritical point in a spin-1/2 zigzag-chain antiferromagnet with anisotropic Γ -term*, *arXiv:2401.06551* (2024).

⁷² A. Ali, S. Elghaayda, S. Al-Kuwari, M. I. Hussain, M. T. Rahim, H. Kuniyil, C. Seida, A. El Allati, and M. Mansour, *Super-extensive scaling of ergotropy in a spin-1/2 XY- Γ chain*, *arXiv:2411.14074* (2024).

⁷³ E. S. Sørensen, J. Gordon, J. Riddell, T. Wang, and H.-Y. Kee, *Field-induced chiral soliton phase in the Kitaev spin chain*, *Phys. Rev. Res.* **5**, L012027 (2023).

⁷⁴ E. S. Sørensen, J. Riddell, and H.-Y. Kee, *Islands of chiral solitons in integer-spin Kitaev chains*, *Phys. Rev. Res.* **5**, 013210 (2023).

⁷⁵ P. Laurell, G. Alvarez, and E. Dagotto, *Spin dynamics of the generalized quantum spin compass chain*, *Phys. Rev. B* **107**, 104414 (2023).

⁷⁶ C. M. Morris, N. Desai, J. Viirok, D. Huvonen, U. Nagel, T. Rööm, J. W. Krizan, R. J. Cava, T. M. McQueen, S. M. Koohpayeh, R. K. Kaul, and N. P. Armitage, *Duality and domain wall dynamics in a twisted Kitaev chain*, *Nat. Phys.* **17**, 832 (2021).

⁷⁷ D. Churchill, H.-Y. Kee, *Transforming from Kitaev to Disguised Ising Chain: Application to $CoNb_2O_6$* , *Phys. Rev. Lett.* **133**, 056703 (2024).

⁷⁸ V. Subrahmanyam, *Block entropy for Kitaev-type spin chains in a transverse field*, *Phys. Rev. A* **88**, 032315 (2013).

⁷⁹ M. Bhullar, *Field-induced ordered phases in anisotropic spin-1/2 Kitaev chains*, *Phys. Rev. B* **111**, 104439 (2025).

⁸⁰ S. Birnkmamer, J. Knolle, and M. Knap, *Signatures of domain-wall confinement in Raman spectroscopy of Ising spin chains*, *Phys. Rev. B* **110**, 134408 (2024).

⁸¹ A. Metavitsiadis and W. Brenig, *Flux mobility delocalization in the Kitaev spin ladder*, *Phys. Rev. B* **103**, 195102 (2021).

⁸² W.-L. You, Y. Wang, and W. Yi, *Quantum coherence in a compass chain under an alternating transverse magnetic field*, *Phys. Rev. B* **97**, 224420 (2018).

⁸³ N. Wu and W.-L. You, *Exact zero modes in a quantum compass chain under transverse fields*, *Phys. Rev. B* **100**, 085130 (2019).

⁸⁴ S. C. Furuya and M. Sato, *Electric-field control of magnetic anisotropies: Applications to Kitaev spin liquids and topological spin textures*, *Phys. Rev. Res.* **6**, 013228 (2024).

⁸⁵ N. Laflorencie, E. S. Sørensen, M.-S. Chang, and I. Affleck, *Boundary Effects in the Critical Scaling of Entanglement Entropy in 1D Systems*, *Phys. Rev. Lett.* **96**, 100603 (2006).

⁸⁶ P. Calabrese and J. Cardy, *Entanglement entropy and conformal field theory*, *J. Phys. A* **42**, 504005 (2009).

⁸⁷ I. Garate and I. Affleck, *Phys. Rev. B* **81**, 144419 (2010).

⁸⁸ S. Gangadharaiah, J. Sun, and O. A. Starykh, *Phys. Rev. B* **78**, 054436 (2008).

⁸⁹ A. P. Schnyder, O. A. Starykh, and L. Balents, *Phys. Rev. B* **78**, 174420 (2008).

⁹⁰ R. Comin, G. Levy, B. Ludbrook, Z.-H. Zhu, C. N. Veenstra, J. A. Rosen, Yogesh Singh, P. Gegenwart, D. Stricker, J. N. Hancock, D. van der Marel, I. S. Elfimov, and A. Damascelli, *Na_2IrO_3 as a Novel Relativistic Mott Insulator with a 340-meV Gap*, *Phys. Rev. Lett.* **109**, 266406 (2012).

⁹¹ Matthew Fishman, Steven R. White, E. Miles Stoudenmire, *The ITensor Software Library for Tensor Network Calculations*, *SciPost Phys. Codebases* **4** (2022).